Metal(loid)s in urban soil from historical municipal solid waste landfill: Geochemistry, source apportionment, bioaccessibility testing and human health risks

Edgar Hiller [a,*], Tomáš Faragó [a], Martin Kolesár [b], Lenka Filová [c], Martin Mihaljevič [d], Ľubomír Jurkovič [a], Rastislav Demko [e], Andrej Machlica [b], Ján Štefánek [b], Martina Vítková [f]

[a] Department of Geochemistry, Faculty of Natural Sciences, Comenius University in Bratislava, Ilkovičova 6, 842 15 Bratislava, Slovak Republic
[b] DEKONTA Slovensko, Ltd., Odeská 49, 821 06 Bratislava, Slovak Republic
[c] Department of Applied Mathematics and Statistics, Faculty of Mathematics, Physics and Informatics, Comenius University in Bratislava, Mlynská dolina 1, 842 48 Bratislava, Slovak Republic
[d] Institute of Geochemistry, Mineralogy and Mineral Resources, Faculty of Science, Charles University, Albertov 6, 128 43 Prague 2, Czech Republic
[e] Department of Older Geological Formations, Division of Geology, State Geological Institute of Dionýz Štúr, Mlynská dolina 1, 817 04 Bratislava 11, Slovak Republic
[f] Department of Environmental Geosciences, Faculty of Environmental Sciences, Czech University of Life Sciences Prague, Kamýcká 129, 165 00, Praha - Suchdol, Czech Republic

HIGHLIGHTS

- Environmental and health impacts of landfill soils in the city centre were assessed.
- Metal (loid) concentrations were unevenly distributed spatially and vertically.
- Metal (loid) bioaccessibility and fractionation differed and correlated mutually.
- Reservoirs of bioaccessible metal (loid)s were calcite and Fe (hydr)oxides.
- Old landfill represents non-carcinogenic health risk to children.

GRAPHICAL ABSTRACT
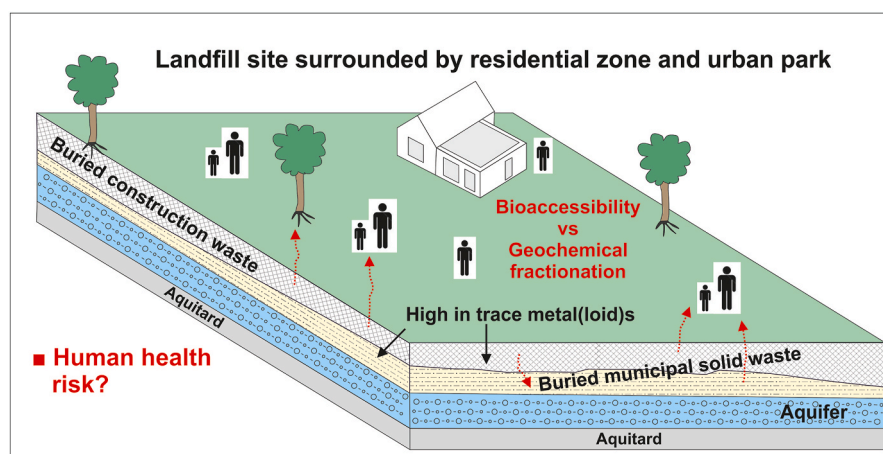
ARTICLE INFO

Handling editor: Lena Q. Ma

ABSTRACT

Landfills, especially those poorly managed, can negatively affect the environment and human beings through chemical contamination of soils and waters. This study investigates the soils of a historical municipal solid waste

* Corresponding author.
E-mail addresses: edgar.hiller@uniba.sk (E. Hiller), tomas.farago@uniba.sk (T. Faragó), martin.kolesar@dekonta.sk (M. Kolesár), lenka.filova@fmph.uniba.sk (L. Filová), martin.mihaljevic@natur.cuni.cz (M. Mihaljevič), lubomir.jurkovic@uniba.sk (Ľ. Jurkovič), rastislav.demko@geology.sk (R. Demko), andrej.machlica@dekonta.sk (A. Machlica), jan.stefanek@dekonta.sk (J. Štefánek), vitkovam@fzp.czu.cz (M. Vítková).

(MSW) landfill situated in the heart of a residential zone in the capital of Slovakia, Bratislava, with an emphasis on metal (loid) contamination and its consequences. Regardless of the depth, many of the soils exhibited high metal (loid) concentrations, mainly Cd, Cu, Pb, Sb, Sn and Zn (up to 24, 2620, 2420, 134, 811 and 6220 mg/kg, respectively), classifying them as extremely contaminated based on the geo-accumulation index ($I_{geo} > 5$). The stable lead isotopic ratios of the landfill topsoil varied widely (1.1679–1.2074 for $^{206}Pb/^{207}Pb$ and 2.0573–2.1111 for $^{208}Pb/^{206}Pb$) and indicated that Pb contained a natural component and an anthropogenic component, likely municipal solid waste incineration (MSWI) ash and construction waste. Oral bioaccessibility of metal (loid)s in the topsoil was variable with Cd (73.2–106%) and Fe (0.98–2.10%) being the most and least bioaccessible, respectively. The variation of metal (loid) bioaccessibility among the soils could be explained by differences in their geochemical fractionation as shown by positive correlations of bioaccessibility values with the first two fractions of BCR (Community Bureau of Reference) sequential extraction for As, Cd, Mn, Ni, Pb, Sn and Zn. The results of geochemical fractionation coupled with the mineralogical characterisation of topsoil showed that the reservoir of bioaccessible metal (loid)s was calcite and Fe (hydr)oxides. Based on *aqua regia* metal (loid) concentrations, a non-carcinogenic risk was demonstrated for children (HI = 1.59) but no risk taking into account their bioaccessible concentrations (HI = 0.65). This study emphasises the need for detailed research of the geochemistry of wastes deposited in urban soils to assess the potentially hazardous sources and determine the actual bioaccessibility and human health risks of the accumulated metal (loid)s.

1. Introduction

Chemical contamination of soils is one of the serious consequences of today's consumer and industrial society and affects all continents (Antoniadis et al., 2019; Binner et al., 2023). The most studied group of chemical contaminants are compounds of trace elements, especially metal (loid)s, such as As, Cd, Cr, Cu, Hg, Ni, Pb, Sb, Zn and others (Kumar et al., 2023; Silva-Gigante et al., 2023; Varol et al., 2020). The reasons for this interest are in their common occurrence in the earth's crust, wide-spectrum industrial applications, numerous natural and anthropogenic sources, persistence and toxicity to living organisms (Bolan et al., 2022; Elnabi et al., 2023). There are numerous anthropogenic sources of metal (loid)s in the urbanised environment, e.g., road transport, industries, building/construction materials, and waste landfills (Adewumi and Ogundele, 2024; Alloway, 2013; Binner et al., 2023; Pecina et al., 2021; Zwolak et al., 2019). Recent studies show that the chemistry of soils is often altered in the vicinity of landfills due to leaching of chemical elements from the deposited waste (de Souza et al., 2023; Gujre et al., 2021; Somani et al., 2020; Wang et al., 2022; Wu et al., 2022). Although the impact of landfills on soil contamination is localised, they can pose health risks to residents living near them (Du and Li, 2023; Karimian et al., 2021; Obiri-Nyarko et al., 2021).

When assessing human health risks due to exposure to metal (loid)s in soils, total concentrations are an essential part of this process and reflect worst-case scenarios (Peña-Fernández et al., 2014; Yang et al., 2023). On the other hand, total concentrations of metal (loid)s do not correspond to their reactivity in soils because they distribute in several soil components of different geochemical stability (Botsou et al., 2022;

Fig. 1. Location of the historical landfill of municipal solid and construction waste and sampling sites of landfill soils.
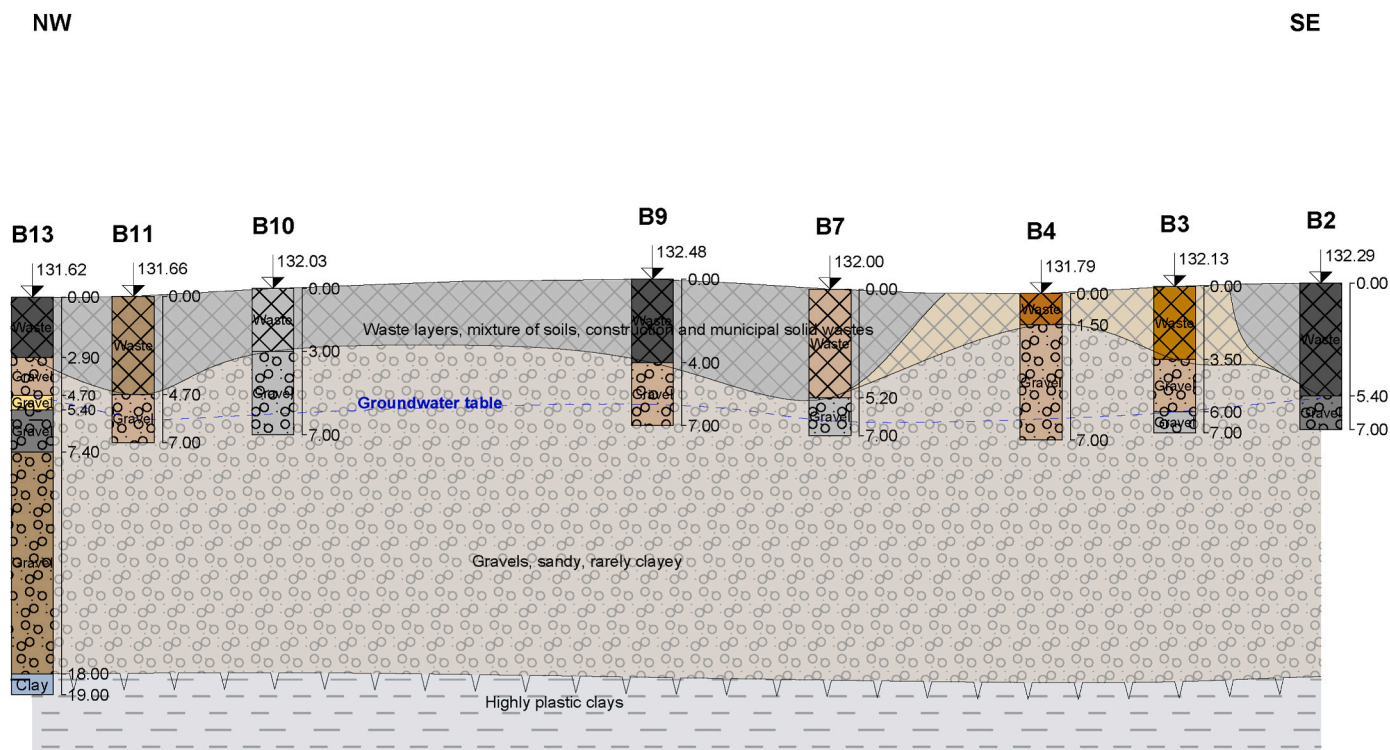
Fig. 2. Lithostratigraphic cross-sectional view in the NW–SE direction of sampling boreholes with the description of core soil samples and marked groundwater level.

Chu et al., 2022; Osibote and Oputu, 2020). To understand the transfer of metal (loid)s from soil to humans, it is important to determine their bioaccessible fractions that reflect the actual solubility in human gastric juices (Billmann et al., 2023; Khan et al., 2023; Roy et al., 2024). To date, there are many bioaccessibility tests that mimic the release of metal (loid)s in the gastrointestinal tract (Li et al., 2016, 2020; Liang et al., 2022), but the most commonly used is the EPA method 1340 (USEPA, 2021) with an acidified glycine solution, i.e., amino acid forming soluble complexes with metals (Dodd et al., 2023, 2024; Kelepertzis and Argyraki, 2015; Kierulf et al., 2022; Kyene et al., 2023; Mendoza et al., 2017). The bioaccessibility of metal (loid)s is related to the physicochemical properties of soils (Billmann et al., 2023; Lu et al., 2023), soil mineralogy (Claes et al., 2023; Drahota et al., 2018; Ettler et al., 2023; Helser et al., 2022) and distribution of metal (loid)s in different soil components (Chu et al., 2022).

There are a number of studies on contamination of landfill soils with metal (loid)s but these investigations mostly considered their total soil concentrations and associated human health risks (Adelopo et al., 2018; Balali et al., 2023; de Souza et al., 2023; Du and Li, 2023; Karimian et al., 2021; Obiri-Nyarko et al., 2021; Zhou et al., 2022), however, rarely addressed other geochemical properties, including bioaccessibility and fractionation, i.e., properties controlling the reactive proportions of metal (loid)s in the human body and soils (Ahmad et al., 2023; Gujre et al., 2021; Wu et al., 2022). Unlike these studies that used one or two methodological approaches to demonstrate contamination of landfill soils with metal (loid)s, this work used a multi-disciplinary approach to further elucidate metal (loid) sources by combining statistical methods and determination of stable lead isotopes as well as their environmental availability using in vitro bioaccessibility testing, geochemical fractionation and mineralogical characterisation. These results are the basis for a more accurate assessment of the human health risk from exposure to metal (loid)s in landfill soils than relying only on their total concentrations. The geochemical results of this study are presented for the soils of a historical landfill used for disposal of municipal, construction waste and municipal solid waste incineration (MSWI) ashes, located in the heart of a residential zone in Bratislava city. These wastes were

deposited in a natural depression and continuously covered with soil. The operation of the landfill ended in the mid-1980s. The unique nature of this area predisposes it to study the impact of deposited waste on soil/groundwater chemistry with an emphasis on trace metal (loid)s. The main driving goal of this study was to assess the human health risks associated with: (i) concentrations of metal (loid)s in soils from different depths, (ii) oral bioaccessibility and geochemical fractionation of metal (loid)s and (iii) mineralogy of selected soils. The results of this study acquire practical significance, especially in connection with the future transformation of the landfill into a residential and recreational zone.

2. Materials and methods

2.1. Description of the study area

The investigated area is a former municipal solid waste (MSW) landfill, which operated from 1967 to 1986. Ashes from the municipal solid waste incineration (MSWI ash) and different construction/demolition wastes were also deposited in the landfill. It is not common practice to dispose of raw municipal solid waste with MSWI ashes, however, at the time of the establishment of the landfill (second half of the 1960s), no measures were taken to prevent this unprecedented practice. It is very likely that the MSWI ash disposed of in this landfill consists of bottom and fly ash. The area is located in the inner city of Bratislava, in the Vrakuňa district and is surrounded by residential zones (Fig. 1). The urban park is located in the southern part of the landfill and widely used by residents. The waste is covered by soil and soil-like material (collectively referred to as landfill soils) but in many places, waste is commonly visible, mainly unsorted municipal solid and construction waste, but also tyres. In some places, the landfill is densely overgrown with invasive vegetation.

The landfill body is located in Quaternary fluvial sediments, which consist of sands and gravels. The gravels are rounded and dominated by quartzites, limestone and crystalline rocks. Irregular layers of fine-grained sands with a thickness of 1–3 m, rarely 5 m, are overlying the gravels. The uppermost layer consists of anthropogenic sediments, i.e.,
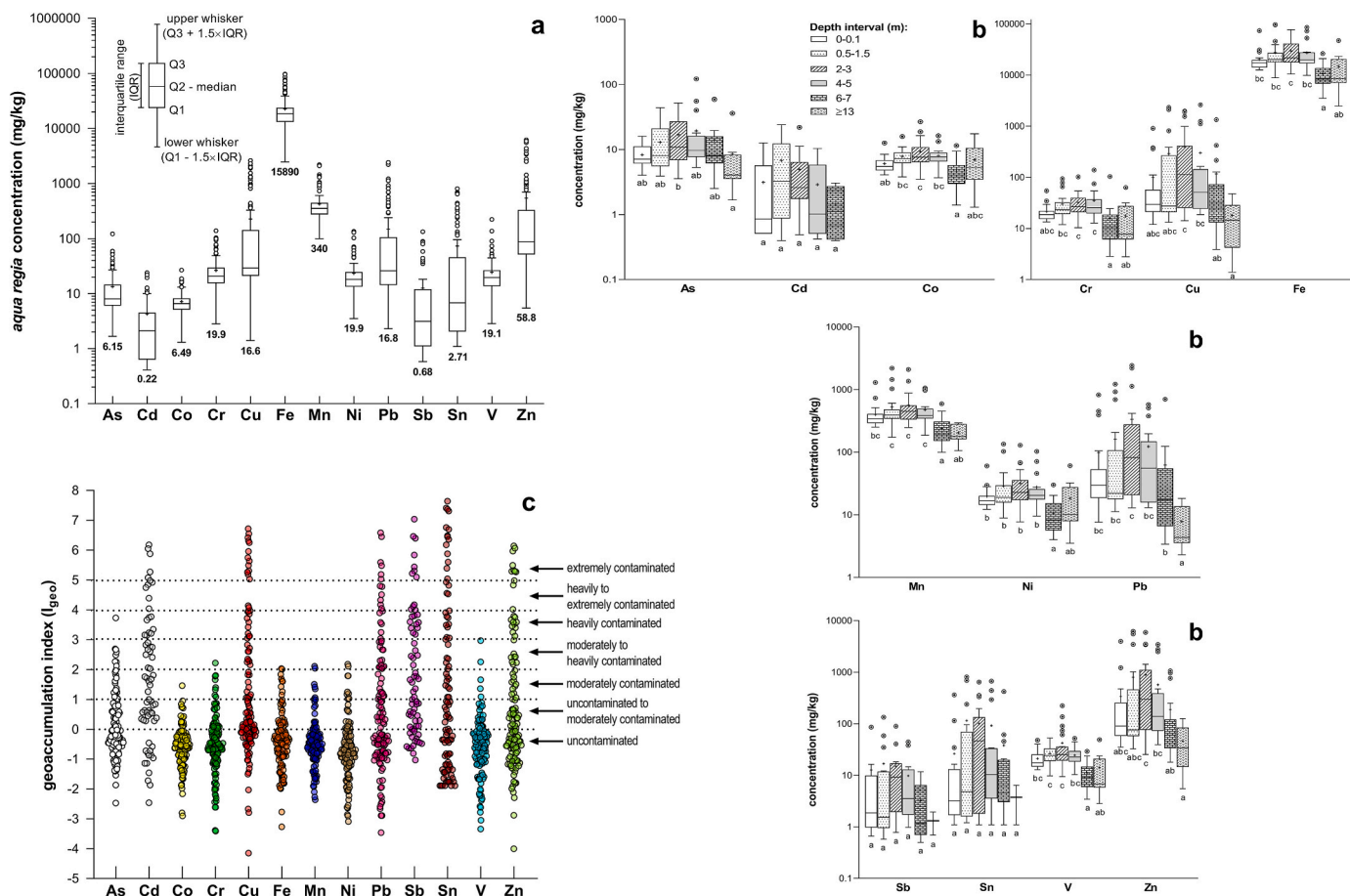
Fig. 3. a) *Aqua regia* concentrations of metal (loid)s in soils of the historical landfill in Bratislava city. Outliers are shown with small white circles and bold numbers below the lower whisker are local background concentrations; **b)** Metal (loid) concentrations in individual sampling depths of 24 boreholes and their statistical comparisons (Kruskal-Wallis test with Dunn's correction). Different lowercase letters below the boxes indicate a significant difference ($p < 0.05$) among the individual depths for each metal (loid) separately; **c)** Individual I_{geo} values.

covering soils and wastes of different composition with a thickness of 1–5 m. The area has a warm and dry climate with a mild winter (Anonymous, 2002). The mean annual temperature is 10.3 °C, with the highest and lowest mean temperature in July (23 °C) and January (−2 °C), respectively. The mean annual precipitation is 600 mm for the years 2002–2018.

2.2. Soil sampling and determination of metal (loid)s and stable lead isotopes

The results are presented for soils from 24 sampling sites as shown in Fig. 1. Surface soil samples (0–0.1 m) at each site were collected from an area of 1 m² by taking 4–5 subsamples using a stainless steel auger (Eijkelkamp), and subsequently mixed to obtain one representative sample from each sampling site. Soil samples from greater depths were obtained by drilling using a UGB 50 type drilling rig. The boreholes were obtained by impact-rotary drilling with a diameter of 180 mm. From the drill cores, samples from the following four depth intervals were selected for chemical analysis: 0.5–1.5 m (zone of biological contact), 2.0–3.0 and 4.0–5.0 m (unsaturated zone), and 6.0–7.0 m (saturated zone). At four sampling sites where permanent wells for groundwater sampling were built (B1, B6, B13 and B16 in Fig. 1), drilling was carried out up to the groundwater aquitard, and the samples were taken from depth intervals of 13–14 m and 15–16 m. In total, 20 out of 24 sampling sites had 5 soils and 4 out of 24 sites had 7 soils, which gives a total of 128 analysed soil samples. Each soil was thoroughly mixed, then air-dried at room temperature, disintegrated and passed through a 2 mm sieve.

Metal (loid) concentrations were determined by inductively coupled plasma-mass spectroscopy (ICP-MS) or atomic emission spectroscopy (ICP-AES) after acid digestion of pulverised soil samples in *aqua regia*. The accuracy and precision of the analytical determination were verified using a certified reference material ERM-CC141 (loam soil). The mean recovery rate was 96.0% for As, 108% for Co, 91.6% for Cr, 103% for Cu, 96.4% for Mn, 90.4% for Ni, 100% for Pb and 92.6% for Zn. Chemical analyses were carried out in accredited laboratories of ALS Slovakia (ALS SK, Ltd. – member of the ALS Limited group).

Lead isotopes (^{206}Pb, ^{207}Pb, and ^{208}Pb) were determined with quadrupole-based ICP-MS (X Series 2, Thermo Scientific) as outlined in the study by Mihaljevič et al. (2011). Briefly, 0.2 g of soil was digested in a mixture of 10 mL of concentrated HF and 0.5 mL HClO₄ in a Pt dish, then evaporated to dryness, and the procedure was repeated with 5 mL HF and 0.5 mL HClO₄. The residue was dissolved in 2 mL HNO₃ and diluted to a volume of 100 mL. To minimise the matrix effect in the determination of Pb isotopes, solutions were purified using the anion exchange resin AG1X8 (details in Ettler et al., 2004). Mass bias was corrected using NIST 981 (common lead) between measurements of individual samples. The accuracy was determined based on analyses of the BCR-2 certified reference material and was within 0.5% RSD (relative standard deviation).

2.3. Geochemical fractionation and bioaccessibility of metal (loid)s

Geochemical fractionation and bioaccessibility of metal (loid)s were tested with eight contrasting landfill topsoils (B1, B4, B6, B10, B13a

Table 1
Comparison of metal (loid) concentrations (all data in mg/kg) between landfill soils of this study and landfill soils from other countries.

Reference	Country	Landfill age (years)[a]	N[b]	Size (mm)	Analytical method	As	Cd	Co	Cr	Cu	Fe	Mn	Ni	Pb	Sb	Sn	V	Zn
This study	Slovakia	45	122	<2	Aqua regia; microwave	13.8 (*8.48*) ±15.3[c] 1.67–122	4.20 (*2.06*) < ±5.62 0.4–24.0	7.19 (*6.62*) ±3.66 1.30–26.8	26.3 (*21.1*) ±21.1 2.81–139	227 (*29.5*) ±497 1.40–2620	22630 (*18500*) ±17720 2470–97200	428 (*353*) ±326 99.6–2200	23.5 (*17.9*) ±21.9 3.50–135	149 (*27.4*) ±355 2.30–2420	11.8 (*2.62* ± 23.2 <0.5–134	72.8 (*6.4*) ±163 <1–811	24.7 (*19.7*) ±25.1 2.83–224	531 (*88.9*) ±1161 5.50–6220
Adamcová et al. (2016)	Czech Republic	20	8	<0.2	Aqua regia; microwave		0.13 ± 0.05	6.80 ± 3.17	86.5 ± 42.7	43.0 ± 9.60		629 ± 52.5	50.8 ± 36.3	5.32 ± 1.73				33.8 ± 5.01
Adelopo et al. (2018)	Lagos	9	12	<6.3	Aqua regia; microwave	2.81 ± 0.02	4.48 ± 1.10	53.3 ± 30.2	26.2 ± 6.35	539 ± 344	11910 ± 609	363 ± 67.0	11.6 ± 3.05	254 ± 46.3				4317 ± 1594
Akoto et al. (2016)	Ghana	NA	20	<2	Aqua regia; microwave			34.4 ± 99.9 3.90–395	122 ± 41.4 63.3–199	91.4 ± 18.3 50.3–108	12590 ± 3923 35–16105			1883 ± 1776 90.0–4846				482 ± 285 91.5–915
Alghamdi et al. (2021)	Saudi Arabia	Active	44	NA	Aqua regia; microwave	1.22 (*0.00*)	0.10 (*0.06*)	9.30 (*9.50*)	16.2 (*15.4*)	20.4 (*19.7*)	6383 (*6522*)	165 (*164*)	16.8 (*16.2*)	4.52 (*4.30*)				69.1 (*64.5*)
Barbieri et al. (2014)	Italy	Active	13	<2	HNO₃–HF–H₂O₂	11.9 (*11.4*) ±5.6	0.08 (*0.04*) ±0.15		16.8 (*17.6*) ±9.90	6.3 (*3.2*) ±7.7	5541 (*6100*) ±3009		10.3 (*8.0*) ±7.3	53.6 (*6.4*) ±143	0.48 (*0.43*) ±0.42		29.0 (*23.3*) ±20.5	25.6 (*16.5*) ±28.5
Critto et al. (2003)	Italy	NA	36	NA	NA	16 ± 14 7–88			10.7 ± 18 5–115	32 ± 76 5–470			17 ± 12 5–85	220 ± 1100 10–6900				1000 ± 5500 25–33000
de Souza et al. (2023)	Brazil	23	20	<0.42	H₂SO₄–HCl					1.78 (*1.80*) ±0.551–3	44.9 (*41.3*) ±22.29.20–93.6	545 (*518*) ±170294–944						21.9 (*20.0*) ±8.30 12.2–48.1
Du and Li (2023)	China	6	376	<0.15	HCl–HNO₃–HF–HClO₄	355 ± 815 0.98–20639	238 ± 380 0.001–2062			2085 ± 910 3.61–49937			392 ± 293 5.92–2513	534 ± 635 3.70–23084	93.7 ± 86.2 0.06–4062			3614 ± 2062 15.8–88009
Gworek et al. (2016)	Poland-	30	6	<1	Aqua regia; microwave		0.33		9.90	5.70			9.20	31.7				32.3
Hölzle (2019)	Germany	landfills of different age	301	<4	Aqua regia; microwave	8; max: 22	*0.9*; max: 5.0		*29*; max: 87	*62*; max: 828			*29*; max: 110	*130*; max: 890				*350*; max: 2800
Hussein et al. (2021)	Malaysia	landfills of different age	NA	<2	Aqua regia; microwave	3.88–163	0.10–1.88		8.38–347	0.40–61.6	16942–58123	10.7–693	0.58–15.6	5.73–172				12.3–96.7
Ihedioha et al. (2017)	Nigeria	Active	240	<2	HNO₃–HClO₄–HF; hot-plate		12.2		4.05		1804	91.2	11.8	8.70				146
Karimian et al. (2021)	Iran	Active		<0.15	HNO₃–HClO₄–HCl	3.9–10.9		10.7–18.0	62.1–128	41.9–179	30542–46364	799–1254	21.4–42.9	18.5–112				59.1–275
Obiri-Nyarko et al. (2021)	Ghana	2	17	<2	HNO₃–HF	196–391				31.5–79.9				14.1–352				145–1876
Osibote and Oputu (2020)	South Africa	landfills of different age	41	<0.25	BCR SEP; *aqua regia*	0.07–0.23	6.99–10.3		53.6–98.4	22.1–43.4			19.0–24.6	0.09–0.12	24.1–44.6			95.6–197

Table 1 (*continued*)

Reference	Country	Landfill age (years)[a]	N[b]	Size (mm)	Analytical method	As	Cd	Co	Cr	Cu	Fe	Mn	Ni	Pb	Sb	Sn	V	Zn
Oyelola and Babatunde (2008)	Nigeria	Active	20	<2	HNO$_3$–HClO$_4$; hot-plate				18.4	64.6			5.99	155				449
Prechthai et al. (2008)	Thailand	25	12	<1	HNO$_3$–H$_2$O$_2$–HCl;		0.9–38		57.3–186	119–545		100–353	24.2–94.0	13.2–127				275–587
Shejjany et al. (2020)	Iran	37	30	<2	HNO$_3$–HClO$_4$–HF–HCl	10.5	0.16		19.1	20.2				25.0				28.8
Somani et al. (2020)	India	landfills of different age	42	<4.75	Aqua regia; microwave	2.58–7.80	0.28–3.76		89.0–339	140–574		125–408	26.2–97.0	27.0–333				153–696
Vongdala et al. (2019)	Laos	Active	48	<0.2	7 M HNO$_3$		3.76 ± 0.33		39.7 ± 3.78	66.8 ± 27.5			19.4 ± 0.84	80.2 ± 19.3				77.5 ± 57.9
Wu et al. (2022)	China	10	68	<2	HNO$_3$–H$_2$O$_2$–HF; microwave	6.13	0.17		43.9	23.9		475	15.9	31.0				95.0
Zhou et al. (2022)	Tibet	Active	72	<0.07	HNO$_3$–H$_2$O$_2$–HF; microwave	27.0 ± 4.89	0.40 ± 0.92		54.6 ± 10.4	30.0 ± 16.1			25.3 ± 5.57	36.4 ± 13.7				84.9 ± 49.5

[a] Age after landfill closure.

[b] Number of soil samples.

[c] Arithmetic mean ± standard deviation; Median, if shown in the cited study, is given in *italics*; Numbers separated by a long space are the range of concentration values (min–max).

(weathered MSWI ash), B16, B18, B24) of size fraction <250 μm and carried out in duplicate. Prior to testing, *aqua regia* metal (loid) concentrations were also measured in <250 μm soil size using the same analytical protocol as for the <2000 μm soil particle size.

To determine the solid-phase speciation of metal (loid)s, a modified BCR (Community Bureau of Reference) sequential extraction procedure was applied, which fractionates chemical elements into four fractions (Rauret et al., 1999): EX1 (exchangeable/carbonate), RED2 (reducible; Fe–Mn oxides), OX3 (oxidisable; organic matter) and RES4 (residual). Firstly, 1 g soil was extracted with 40 mL of 0.11 *M* acetic acid solution by shaking in an end-over-end shaker (30 ± 5 rpm) for 16 h at 22 ± 2 °C. The extract was separated by centrifugation (3000 *g* for 20 min), collected in PE bottles and stored at 4 °C until analysis. The residue was washed by shaking for 15 min with 20 mL of deionised water and then centrifuged. In the second step, the soil was extracted with 40 mL of 0.5 *M* hydroxylammonium chloride solution and further processed as in the first step. Third step was as follows: the soil residue was mixed with 10 mL of 8.8 *M* hydrogen peroxide solution and sequentially extracted for 1 h at 22 ± 2 °C and for 1 h at 85 ± 2 °C, and then the volume was reduced to <2 mL. A second aliquot of 10 mL H$_2$O$_2$ was added, extracted again for 1 h at 85 ± 2 °C, and reduced to ~1 mL. The residue was extracted with 50 mL of 1 *M* ammonium acetate solution at pH 2.0 under the same conditions as in the first two steps. The separated and washed residue from the third step was digested with *aqua regia* according to ISO 54321:2020 (ISO, 2020). It should be noted that BCR sequential extraction is not the most suitable for metalloids, As and Sb, but it was used in order to compare their fractionation to the investigated metals.

The EPA method 1340 (USEPA, 2021) used to determine the gastric bioaccessibility of metal (loid)s included a 1 h extraction of soil samples in HDPE tubes with a 0.4 *M* glycine solution with pH = 1.5 ± 0.1 at a soil:solution ratio of 1:100 (w/v) and a temperature of 37 ± 2 °C. Extracts were then filtered through a 0.45 μm membrane filter, diluted and analysed for bioaccessible metal (loid) concentrations using ICP-MS. The accuracy of the analytical determinations in extracts was controlled by analyses of the standard reference material NIST SRM 1640a (Trace elements in natural water). The recovery of the target metal (loid)s was within 92–99%.

2.4. Mineralogy

Samples from four sampling sites (B6, B13a (weathered MSWI ash), B13b (soil with high proportion of MSWI ash), B10, B16) were selected for the mineralogical study. The main minerals were detected by X-ray diffraction (XRD; Philips PW 1710 diffractometer, graphite monochromator, Cu Kα radiation, 40 kV, 20 mA, 2θ range 4–80°, 0.02° step, 1 s/step). The diffraction data were interpreted based on the Rietveld refinement using the X'pert Highscore Plus 2.0.1 software.

The chemical composition of selected grains was measured by electron microprobe analyser (EMP; Cameca SX100) equipped with wavelength-dispersive X-ray (WDS) detector. The details of the measuring conditions, standards, X-ray lines and detection limits are listed in Table S1. Moreover, scanning electron microscopy (TESCAN VEGA3XMU, Czech Republic) equipped with a Bruker QUANTAX200 energy dispersive X-ray spectrometer (EDS) was used for imaging and semi-quantitative chemical analyses of calcite grains.

Raman spectroscopy (Thermo Scientific DXR3xi Raman Imaging Microscope) was used for mineral identification of selected grains. Photographs of micro- and macro-particles were obtained with a Leica DVM6 digital microscope.

2.5. Data analysis and human health risk assessment

Descriptive statistical parameters of metal (loid) concentrations, including arithmetic mean, standard deviation (SD), median, 25% and 75% percentiles, range and coefficient of variation (CV), were calculated and outliers were identified. Due to compositional nature of
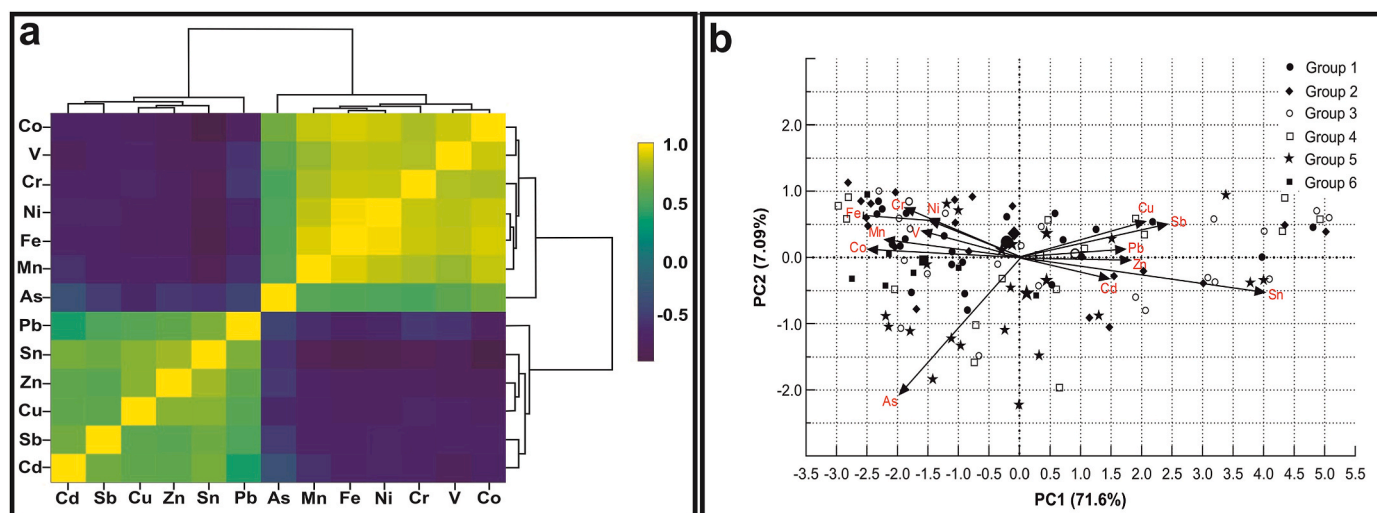
Fig. 4. a) Heat-map of the correlation coefficients based on symmetric balances together with the results of the cluster analysis and **b)** rotated biplot of the first two principal components according to the *clr*-PCA results. Groups 1, 2, 3, 4, 5 and 6 in Figure **b)** include soils from depth intervals of 0–0.1, 0.5–1.5, 2–3, 4–5, 6–7 and ≥13 m, respectively.

geochemical data, a correlation coefficient based on log-ratio transformations was used to evaluate the relationships between pairs of metal (loid)s (Kynčlová et al., 2017; Reimann et al., 2017). Principal component analysis after *centred log-ratio* (*clr*) transformation of the concentration data (*clr*-PCA) was carried out to reduce the number of variables, and to identify sources and similarities of metal (loid)s in soils. The R software and GraphPad Prism, version 8.0.1 were used for data processing.

The degree of soil contamination was estimated through the geo-accumulation index (I_{geo}) using the equation:

$$I_{geo} = log_2(C_n/1.5 \times B_n)$$

where the factor 1.5 expresses the variation of background values due to lithogenic effects, C_n is the measured concentration of metal (loid) in soil and B_n is the background concentration of the same metal (loid). According to I_{geo}, the degree of soil contamination is classified into seven classes (Müller, 1979): $I_{geo} \leq 0$ = uncontaminated, $0 < I_{geo} \leq 1$ = uncontaminated to moderately contaminated, $1 < I_{geo} \leq 2$ = moderately contaminated, $2 < I_{geo} \leq 3$ = moderately to heavily contaminated, $3 < I_{geo} \leq 4$ = heavily contaminated, $4 < I_{geo} \leq 5$ = heavily to extremely contaminated and $I_{geo} > 5$ = extremely contaminated. The mean *aqua regia* metal (loid) concentrations from ten local soils collected in relatively undisturbed areas of Bratislava city were considered as background values for the calculation of I_{geo} values. The background concentrations (in mg/kg) were: 6.15 (As), 0.22 (Cd), 6.49 (Co), 19.9 (Cr), 16.6 (Cu), 15890 (Fe), 340 (Mn), 19.9 (Ni), 16.8 (Pb), 0.68 (Sb), 2.71 (Sn), 19.1 (V) and 58.8 (Zn). To infer the natural source of Pb, the same soils were also analysed for Pb isotopic ratios.

The exposure scenario considered the recreational activities of children/adults after the complete reclamation of the landfill who are exposed to metal (loid)s through three exposure routes: (i) soil ingestion, (ii) dermal contact and (iii) dust inhalation. A possible worst-case scenario considered was that the person was in contact with shallowly buried soil-waste layers that would be exposed after landscaping and levelling. The values of the 95% upper confidence limit of the mean calculated by the ProUCL software (USEPA, 2022) were taken as point exposure concentrations of metal (loid)s. For soil ingestion, non-carcinogenic and carcinogenic risks were calculated for two scenarios: (i) the relative metal (loid) bioavailability (RBA) was 100%, and (ii) RBA corresponded to the mean value of the gastric bioaccessibility of the respective metal (loid). Chronic daily intakes (CDI) and lifetime average daily doses (LADD) of metal (loid)s for non-carcinogenic and

carcinogenic risk assessment, respectively, were calculated using the Chemical Risk Calculator (RAIS, 2023). The equations are given in Supplementary text S1 and the values of the input exposure parameters are in Table S2.

Non-carcinogenic risk was quantified using the hazard quotient (HQ, dimensionless) for individual exposure routes as follows:

$$HQ_{ingestion} = CDI_{ingestion}/RfD_o \qquad (1)$$

$$HQ_{inhalation} = CDI_{inhalation}/RfC \qquad (2)$$

$$HQ_{dermal\ contact} = CDI_{dermal\ contact}/RfD_d \qquad (3)$$

where RfD_o (mg/kg.d), RfC (mg/m^3) and RfD_d (mg/kg.d) are the oral reference dose, reference inhalation concentration and the dermal reference dose, respectively. The HQ values for each determined metal (loid) were summed to obtain the total risk, quantified using the hazard index of the individual metal (loid) (HI_i):

$$HI_i = HQ_{ingestion} + HQ_{inhalation} + HQ_{dermal\ contact} \qquad (4)$$

The hazard index of each metal (loid) can be further summed, which then expresses the total (cumulative) risk of all determined metal (loid)s (HI_{total}):

$$HI_{total} = \sum HI_i \qquad (5)$$

When HQ or HI < 1.0, no non-carcinogenic health effects exist, while HQ or HI > 1.0 indicates the existence of non-carcinogenic risk.

Carcinogenic risk was quantified using the cancer risk (CR, dimensionless) as follows:

$$CR_{ingestion} = LADD_{ingestion} \times OSF \qquad (6)$$

$$CR_{inhalation} = LADD_{inhalation} \times IUR \qquad (7)$$

$$CR_{dermal\ contact} = LADD_{dermal\ contact} \times DSF \qquad (8)$$

where OSF (1/(mg/kg.d)), IUR (1/(mg/m^3)) and DSF (1/(mg/kg.d)) are the oral slope factor, inhalation unit risk and dermal slope factor, respectively. The cancer risk of each metal (loid) (CR_i) was calculated as the sum of the CR values for all three exposure routes:

$$CR_i = CR_{ingestion} + CR_{inhalation} + CR_{dermal\ contact} \qquad (9)$$

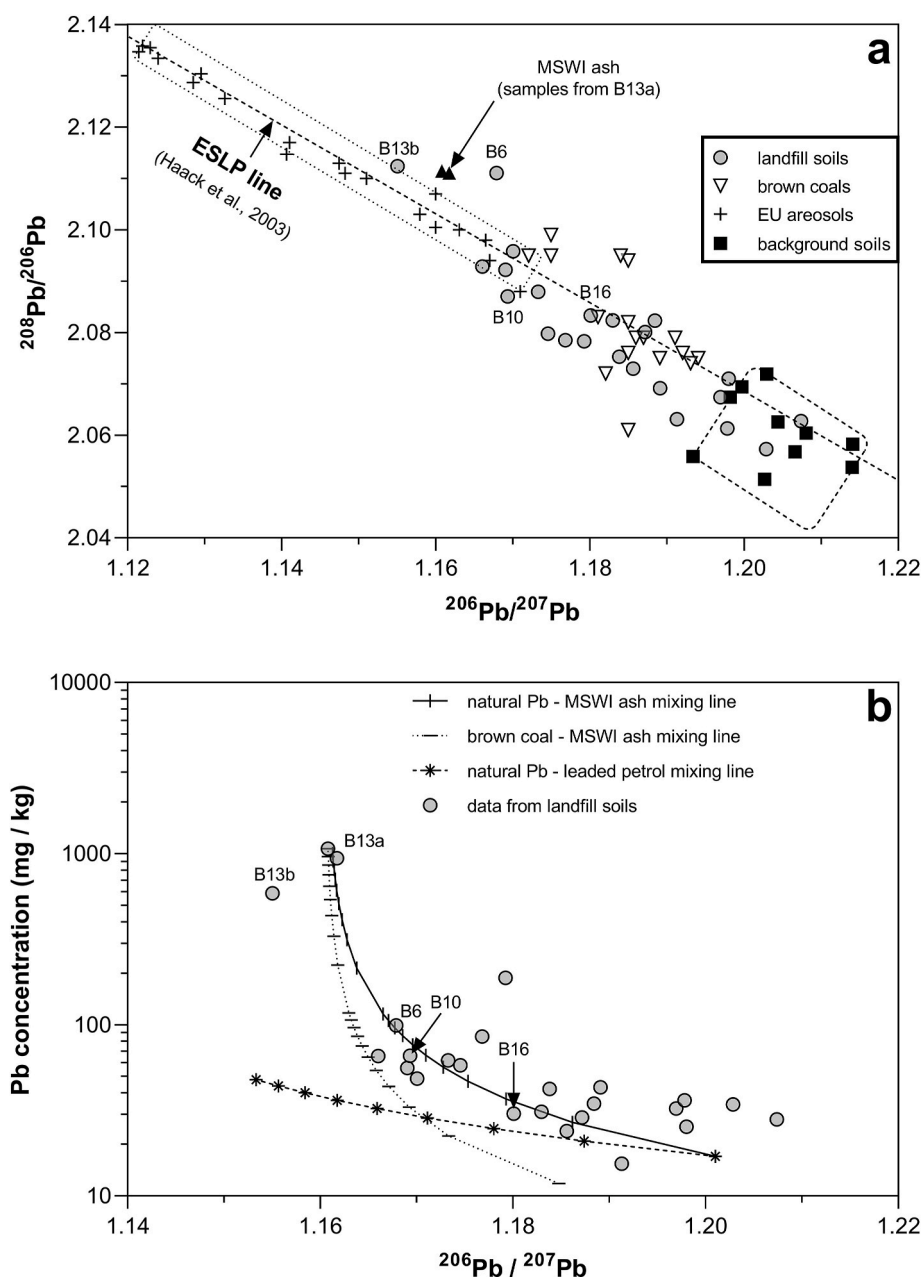Combined cancer risk of all carcinogenic metal (loid)s (CR_{total}) was

Fig. 5. a) Lead isotopic composition of landfill soils (grey circles). The European Standard Lead Pollution line (ESLP) was calculated according to the equation derived in the study by Haack et al. (2003). Data on EU aerosols, brown coals and background soils were taken from Hamelin et al. (1997), Hansmann and Köppel, 2000, Mihaljevič et al. (2009) and Hiller et al. (2021), respectively; **b)** Curves calculated according to the equation presented in the study of Tyszka et al. (2016) representing a simple two-component mixing model and taking the most likely sources of Pb into landfill soils, such as natural Pb source and anthropogenic sources: MSWI ash, leaded gasoline, and Czech brown coals. The symbols on the modelled curves indicate 1% steps (first 10 symbols) and 10% steps (remaining 10 symbols). For natural Pb – leaded petrol mixing line, only the first eight 1% increments are shown. Labeled samples (B6, B10, B13a, b and B16 were subjected to mineralogy.

then calculated as follows:

$$CR_{total} = \sum CR_i \qquad (10)$$

Carcinogenic metal (loid)s via soil ingestion and dermal contact are As and Pb, while the IUR is also defined for Cd, Co and Ni. The physical meaning of CR is that the CR value of 10^{-n} indicates the carcinogenic risk of one additional person out of a group of 10^n persons. An unacceptable carcinogenic risk is when $CR > 10^{-4}$, CR values between 10^{-4}–10^{-6} are in an acceptable risk, while CR values $< 10^{-6}$ indicate no significant carcinogenic risk. Chemical toxicity values for the metal (loid)s are listed in Table S3.

3. Results and discussion

3.1. Metal (loid)s in soils and source apportionment

Selected geological section with NW-SE orientation and lithostratigraphic profiles of sampling sites B2, B3, B4, B7, B9, B10, B11 and B13 are shown in Fig. 2. It is clear from Fig. 2 and visual inspection of the drilled cores (Fig. S1) that waste is buried in different depths, mostly 0.5 up to 5 m below the ground surface. The waste layers represented soil-like material, although waste residues were still distinguishable in these layers. The soils on the surface were mixed with municipal and construction waste as well as incineration waste products, i.e., MSWI ash (Fig. S2).
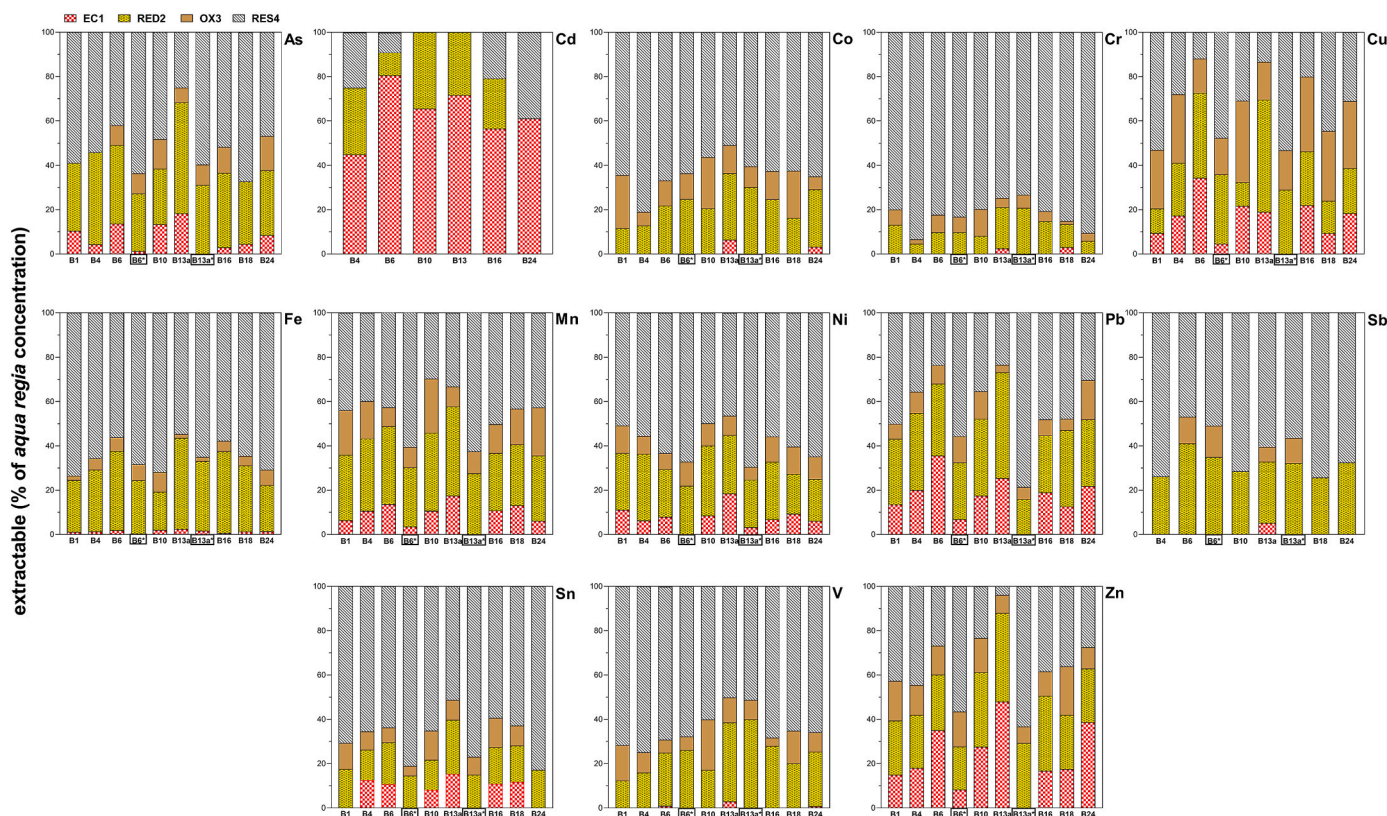
Fig. 6. Fractionation of metal (loid)s in landfill soils according to BCR sequential extraction procedure. Samples marked with asterisk (B6* and B13a*) and boxed represent the geochemical fractionation of metal (loid)s after bioaccessibility testing. Cadmium is not shown because the extracted Cd concentrations were below the detection limit after bioaccessibility testing.

Aqua regia concentrations of several metal (loid)s (i.e., As, Cd, Cu, Pb, Sb, Sn and Zn) in landfill soils, regardless of sampling depth and site, exhibited considerable variation with CV values > 200% in many cases (Fig. 3a; Table S4). For example, Cu, Pb, Sb, Sn and Zn concentrations (in mg/kg) varied up to three orders of magnitude, between 1.40 and 2620, 2.30–2420, <0.50–134, <1.0–811 and 5.50–6220, respectively. The concentrations of other metals (Co, Cr, Fe, Mn, Ni and V) fluctuated less compared to those mentioned above (Fig. 3a).

The highest metal (loid) concentrations contained soil–waste layers with a median of 13.7 (As), 2.34 (Cd), 8.18 (Co), 32.0 (Cr), 248 (Cu), 28250 (Fe), 503 (Mn), 28.7 (Ni), 181 (Pb), 9.97 (Sb), 50.5 (Sn), 27.1 (V) and 493 (Zn) mg/kg, while Cd, Cu, Pb, Sb, Sn and Zn exceeded many times the background values (Fig. 3a). Considering each metal (loid) in individual sampling depths, the lowest concentrations exhibited commonly aquitard sediments (≥13 m) and soils of the saturated zone in a depth of 6–7 m; however, compared to other depths, the concentration differences were not significant for all metal (loid) (Fig. 3b). On the contrary and as mentioned above, the highest metal (loid) concentrations contained shallower soils (mainly in depth intervals 0.5–1.5 and 2–3 m) with a clear presence of wastes. The variability of metal (loid) concentration could be attributed to the uneven distribution of waste in the landfill, which leads to different mass ratios of soil to deposited waste, different types of deposited waste and proportions of several types of waste at individual sampling points. Uneven spatial and vertical distribution of metal (loid) concentrations is typical for landfill soils (Wang et al., 2022; Wu et al., 2022).

A comparison of the studied landfill with others from different countries of the world (Table 1) showed that the detected metal (loid) concentrations were within the entire range of those in the soils of the compared landfills, however, the variability of metalloid concentrations remains extensive (Hölzle, 2019; Hölzle et al., 2022; Wang et al., 2022). These concentration differences among the landfills relate primarily to

the type of waste, its composition, age of waste accumulation and local geology (Hölzle et al., 2022). Mean concentrations of some metal (loid)s, e.g., As, Cd, Cu, Pb or Zn, with a few exceptions, were rather at the upper end of most compared landfills (Table 1), which could be due to the presence of MSWI ashes that accumulate high concentrations of refractory metal (loid)s (Luo et al., 2019). Du and Li (2023) published unusually high concentrations of metal (loid)s in the soils of the landfill near Baoding city (China) compared to other landfills, which could be related to the fact that the landfill was also used for disposal of wastes from heavy industry.

Based on the calculated I_{geo} values (Fig. 3c), the investigated thirteen metal (loid)s were divided into two main associations: the first association included Co, Cr, Fe, Mn, Ni and V, and the second association consisted of Cd, Cu, Pb, Sb, Sn and Zn. Arsenic had a separate position. The first metal association exhibited the uncontaminated category in most soils, while only a small number of soil samples could be classified as the moderately contaminated category ($1 < I_{geo} \leq 2$). Manganese, Ni, V and Cr only in two and one soils reached moderately to heavily contaminated category, respectively. On the other hand, the second, metal (loid) association fell into all contamination categories defined by I_{geo} values. For Cu and Sn, more than 10% of all soils belonged to the extremely contaminated category ($I_{geo} > 5$), while the highest I_{geo} values had Sn in three soils ($I_{geo} \approx 7–8$). It is interesting to note that Sn is rarely determined in landfill soils, which contradicts its widespread use in the production of tin-plated food and beverage cans, containers, electrical equipment, and construction and glass materials (Kabata-Pendias and Mukherjee, 2007). The low contamination category of the first association (Co, Cr, Fe, Mn, Ni, V) documents the similarity of their concentrations to, or the fact that they are lower than the respective background concentrations. This finding is consistent with Hölzle et al. (2022) who reviewed the concentrations of selected metal (loid)s in soil-like material from 59 landfills of municipal solid and construction
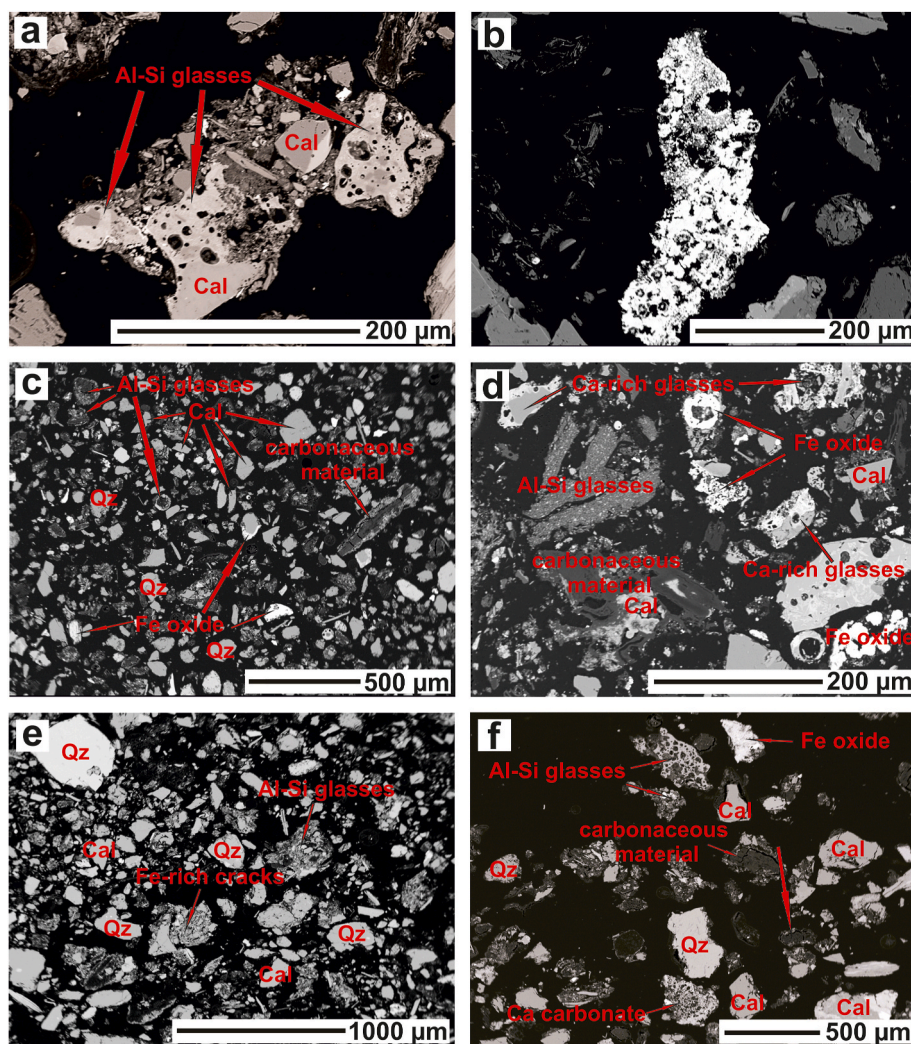
Fig. 7. Back-scattered electron (BSE) micrographs of selected landfill soils (size fraction <250 μm). **a)** An aggregate of vesicular glasses (44–64 wt% SiO$_2$, 12–18 wt% Al$_2$O$_3$, 0.3–16 wt% CaO, 3–16 wt% K$_2$O) and calcite (Cal) cemented with a Ca-rich phase (sample **B6**), **b)** Fe (hydr)oxide (~72 wt% Fe) in soil **B6**, **c)** a mixture of abundant quartz (Qz), glass phases and calcite in MSWI ash–soil (**B13b**), **d)** Weathered MSWI ash (**B13a**) containing mainly glasses with vesicles, quartz (Qz), calcite (Cal), Fe (hydr)oxides and carbonaceous material (up to 1.9 wt% CuO, 3.3 wt% ZnO and 0.3 wt% PbO), **e)** and **f)** Dominant solid phases (quartz, calcite, Fe oxides and glasses) in soils **B16** and **B10**, respectively.

waste and found that Cr and Ni had mostly lower concentrations compared to the abundance in the Earth's crust, but As, Cd, Cu, Pb and Zn concentrations in the soil material exceeded those in the Earth's crust.

The statistical methods used in this study provided comparable results (Fig. 4) and were in accordance with the grouping of metal (loid)s according to I$_{geo}$ values. In general, there were positive correlations between pairs of the metal group Co/Cr/Fe/Mn/Ni/V and between pairs from the group of Cd/Cu/Pb/Sb/Sn/Zn (yellow-green mosaics in Fig. 4a), but the former negatively correlated with the latter (blue colouring in Fig. 4a). The heatmap linked to the dendrogram indicated that the metal (loid)s clustered into the two groups, which was further confirmed by *clr*-PCA. Approximately 79% of the total variation was captured by the first two components (PC1 = 71.6% and PC2 = 7.09%) (Fig. 4b), and the biplot showed two main associations. The first association showed positive loading PC1 and consisted of Cd, Cu, Pb, Sb, Sn and Zn. The second association represented metals towards the negative PC1 with Co, Cr, Fe, Mn, Ni and V. Arsenic was more correlated with PC2 as shown by high negative loadings value on PC2 (Table S5), suggesting no relationship with other metal (loid)s. The first association could reflect not only common occurrence of Cd, Cu, Pb, Sb, Sn and Zn in unsorted solid wastes (Hölzle, 2019,2022) but also the fact that these

metal (loid)s are typical industrial and traffic contaminants of urban areas (Binner et al., 2023). The second association reflected likely natural sources as frequently observed in other urban areas (Binner et al., 2023), including Bratislava city (Hiller et al., 2017; 2021, 2022). However, it was noted that these metals also showed increased concentrations but with much lower frequency, CV and I$_{geo}$ values (Fig. 3; Table S4). In addition, samples less affected by buried waste (i.e., groups 5 and 6 in Fig. 4b) were mostly projected in the lower left quadrant of the biplot, while shallower soils, more affected by waste, were scattered in the remaining quadrants of the biplot depending on the concentration of the particular metal (loid).

3.2. Stable lead isotopes

Topsoil samples were characterised for Pb isotopic composition to further trace the source reservoirs of Pb in a highly altered urban area. The stable Pb isotopic ratios in topsoil varied between 1.1679 and 1.2074 for ^{206}Pb/^{207}Pb and 2.0573–2.1111 for ^{208}Pb/^{206}Pb (Fig. 5a), and plotted along the European Standard Lead Pollution (ESLP) line (Haack et al., 2003). This ESLP line approximates a two-component mixing of radiogenic (higher ^{206}Pb/^{207}Pb ratios typical for natural Pb) and non-radiogenic end members (lower ^{206}Pb/^{207}Pb ratios typical for

Table 2

Electron microprobe (EMP) analyses of selected constituents in the soil samples (sample B6, B10, B13a, B13b, B16). The data are presented in wt%.

	Fe (hydr)oxides ($n = 42$)	Glasses ($n = 51$)	Ash (carbonaceous material) ($n = 6$)	Calcite-rich cements ($n = 10$)	Calcite ($n = 15$)
SiO_2	4.85 (4.30)	38.4 (10.3)	1.11 (1.54)	4.82 (6.91)	BDL
Al_2O_3	3.01 (2.44)	17.4 (7.98)	1.03 (1.33)	2.47 (1.99)	0.08 (0.13)
FeO	67.6 (17.7)	7.89 (8.84)	0.45 (0.61)	5.42 (5.98)	0.06 (0.08)
CaO	1.19 (1.68)	8.48 (8.14)	11.8 (10.2)	49.7 (17.8)	52.7 (7.34)
MgO	0.37 (1.09)	2.78 (2.21)	0.87 (0.47)	0.80 (0.72)	0.31 (0.22)
K_2O	0.23 (0.26)	2.85 (2.87)	0.20 (0.11)	0.20 (0.29)	0.04 (0.05)
MnO	0.25 (0.45)	0.13 (0.19)	0.04 (0.06)	0.58 (0.69)	0.03 (0.04)
As_2O_5	0.05 (0.46)	0.14 (0.25)	BDL [a]	BDL	0.08 (0.04)
CdO	0.01 (0.01)	0.02 (0.01)	BDL	0.07 (0.11)	0.09 (0.06)
CoO	0.06 (0.07)	0.02 (0.02)	BDL	0.02 (0.01)	0.04 (0.02)
Cr_2O_3	0.02 (0.34)	0.04 (0.07)	0.04 (0.05)	0.02 (0.01)	BDL
CuO	0.09 (0.15)	0.07 (0.13)	0.67 (0.74)	0.04 (0.03)	0.35 (0.20)
NiO	0.01 (0.02)	0.02 (0.02)	0.02 (0.01)	0.01 (0.01)	0.11 (0.09)
PbO	0.20 (0.35)	0.68 (3.42)	0.21 (0.09)	0.40 (0.41)	0.47 (0.23)
Sb_2O_3	0.03	0.45 (1.20)	0.02 (0.02)	0.07 (0.05)	0.04 (0.01)
SnO_2	0.05 (0.56)	0.03 (0.03)	0.03 (0.02)	0.24 (0.43)	0.17 (0.11)
ZnO	0.84 (0.89)	0.45 (1.20)	1.20 (1.27)	2.14 (2.44)	1.63 (0.45)
P_2O_5	0.40 (0.46)	0.78 (1.34)	0.43 (0.72)	0.80 (0.75)	0.08 (0.05)
SO_3	0.31 (1.29)	0.18 (0.20)	0.53 (0.41)	0.73 (0.71)	0.35 (0.37)

[a] BDL = below the detection limit of EMP instrument.

anthropogenic sources) that are not always easily distinguishable from each other because they often have a similar range of Pb isotopic ratios (Haack et al., 2003). It can be inferred from Fig. 5a that Pb in the landfill topsoil was derived from natural background and anthropogenic sources but these are difficult to distinguish due to the overlap of their Pb isotopic composition with that of the topsoil. However, it can be expected that the main anthropogenic source of Pb in these soils is deposited solid municipal and construction wastes, which release Pb through long-term weathering, and MSWI ashes containing high Pb concentrations and low, less radiogenic $^{206}Pb/^{207}Pb$ ratios. To help identify the different Pb sources, Pb isotopic compositions of the soils were plotted against the total Pb concentration and compared to its presumed sources (Fig. 5b). Lead isotopic profiles of landfill soils were best described by a curve representing two-component mixing of natural Pb and anthropogenic Pb in MSWI ash. The results coincided separately for soils with lower $^{206}Pb/^{207}Pb$ ratios or high $^{206}Pb/^{207}Pb$ ratios, suggesting that Pb in these soils is the result of mixing of natural Pb and MSWI ash. This is also supported by the mineralogy of the soils (soils B6, B10, B13b, B16), which all contained mineral phases, e.g., Si–Al glasses and carbonaceous material like MSWI ash (B13a), despite the different Pb concentration (see section 3.3). On the other hand, several soils with higher $^{206}Pb/^{207}Pb$ ratios and intermediate Pb concentrations did not fit the

Table 3

Gastric bioaccessible fractions (% of *aqua regia* concentration) and concentrations (mg/kg) of metal (loid)s in landfill soils (particle size <250 µm) at an old landfill in Bratislava city (Slovakia). Arithmetic mean ± standard deviation ($n = 2$). Initial soil pH, organic carbon content (OC; wt%) and calcite abundance (wt%) are also shown.

	B1	B4	B6	B10	B13[a]	B16	B18	B24
pH	7.01 ± 0.06	7.39 ± 0.02	7.47 ± 0.03	7.44 ± 0.03	8.37 ± 0.08	7.08 ± 0.00	7.18 ± 0.06	7.09 ± 0.01
OC	4.27 ± 1.01	2.55 ± 0.30	2.26 ± 0.20	7.27 ± 0.10	4.31 ± 0.21	2.16 ± 0.13	3.56 ± 0.37	2.59 ± 0.08
Calcite	–	–	7	2	11	3	–	–
Bioaccessible fractions (%)								
As	34.7 ± 0.89	34.8 ± 3.64	47.5 ± 2.25	41.7 ± 3.94	69.1 ± 0.73	29.8 ± 4.01	33.4 ± 5.67	22.8 ± 1.89
Cd	NA	73.2 ± 0.00	92.2 ± 6.87	77.9 ± 0.00	106 ± 5.34	76.9 ± 0.00	NA	87.0 ± 0.00
Co	6.06 ± 0.57	6.24 ± 1.26	7.91 ± 0.00	8.68 ± 0.65	10.8 ± 1.51	6.57 ± 0.00	5.34 ± 0.84	5.76 ± 0.43
Cr	1.77 ± 0.00	2.43 ± 0.26	2.53 ± 0.17	3.17 ± 0.00	13.0 ± 0.57	2.28 ± 0.36	1.82 ± 0.00	1.32 ± 0.00
Cu	32.3 ± 0.26	32.7 ± 1.19	60.5 ± 8.38	27.9 ± 0.76	73.4 ± 2.17	31.1 ± 0.45	36.6 ± 1.16	32.3 ± 0.19
Fe	1.60 ± 0.03	1.32 ± 0.05	1.32 ± 0.03	1.23 ± 0.15	2.09 ± 0.06	0.95 ± 0.02	1.27 ± 0.02	1.00 ± 0.02
Mn	33.4 ± 0.86	36.5 ± 1.83	37.1 ± 1.59	38.0 ± 0.21	42.0 ± 1.34	37.6 ± 0.39	35.2 ± 0.63	29.2 ± 0.31
Ni	11.9 ± 0.00	9.26 ± 4.36	8.51 ± 0.00	16.2 ± 0.00	31.8 ± 1.22	11.5 ± 0.00	9.57 ± 0.00	8.43 ± 0.00
Pb	32.8 ± 0.00	46.5 ± 3.86	58.1 ± 2.22	45.5 ± 0.99	79.4 ± 1.95	36.7 ± 2.47	54.2 ± 14.1	47.6 ± 0.00
Sb	NA	13.7 ± 0.00	22.1 ± 0.00	18.3 ± 0.00	14.5 ± 0.06	NA	NA	15.8 ± 7.44
Sn	NA	16.2 ± 1.09	19.8 ± 0.56	12.2 ± 1.67	24.9 ± 3.44	15.8 ± 0.00	18.8 ± 2.95	NA
V	3.87 ± 0.36	5.17 ± 1.46	5.50 ± 0.65	6.18 ± 0.42	9.02 ± 0.38	3.65 ± 0.74	6.42 ± 0.00	3.49 ± 0.55
Zn	16.6 ± 6.22	28.3 ± 1.43	54.3 ± 3.80	71.5 ± 0.00	80.4 ± 3.42	26.0 ± 0.40	34.3 ± 1.82	60.2 0.47
Bioaccessible concentrations (mg/kg)								
As	2.75 ± 0.07	2.70 ± 0.28	7.45 ± 0.35	2.25 ± 0.21	13.4 ± 0.14	2.10 ± 0.28	2.50 ± 0.42	2.55 ± 0.21
Cd	NA	0.30 ± 0.00	0.95 ± 0.07	0.60 ± 0.00	18.3 ± 0.92	0.20 ± 0.00	NA	0.20 ± 0.00
Co	0.38 ± 0.04	0.35 ± 0.07	0.70 ± 0.00	0.38 ± 0.03	1.11 ± 0.16	0.40 ± 0.00	0.45 ± 0.07	0.95 ± 0.08
Cr	0.40 ± 0.00	0.65 ± 0.07	1.05 ± 0.07	1.00 ± 0.00	11.2 ± 0.49	0.45 ± 0.07	0.50 ± 0.00	0.40 ± 0.00
Cu	8.65 ± 0.07	17.6 ± 0.64	51.6 ± 7.14	20.7 ± 0.57	728 ± 21.5	9.80 ± 0.14	11.2 ± 0.35	11.8 ± 0.07
Fe	328 ± 6.15	241 ± 9.76	409 ± 7.99	228 ± 28.5	1783 ± 53.7	165 ± 2.62	253 ± 3.25	348 ± 5.73
Mn	197 ± 5.09	149 ± 7.50	159 ± 6.79	234 ± 1.27	717 ± 22.8	170 ± 1.77	187 ± 3.32	192 ± 2.05
Ni	2.00 ± 0.00	1.50 ± 0.00	2.00 ± 0.00	3.00 ± 0.00	18.5 ± 0.71	2.00 ± 0.00	2.00 ± 0.01	3.00 ± 0.00
Pb	10.0 ± 0.00	25.5 ± 2.12	37.0 ± 1.41	32.5 ± 0.71	834 ± 20.5	10.5 ± 0.71	24.5 ± 6.36	14.0 ± 0.00
Sb	NA	0.30 ± 0.00	0.90 ± 0.00	0.30 ± 0.21	16.1 ± 0.07	NA	NA	0.15 ± 0.07
Sn	NA	1.05 ± 0.07	7.55 ± 0.21	1.55 ± 0.21	82.0 ± 11.3	0.60 ± 0.00	0.45 ± 0.07	NA
V	0.75 ± 0.07	0.75 ± 0.21	2.40 ± 0.28	1.05 ± 0.07	3.40 ± 0.14	0.70 ± 0.14	1.40 ± 0.00	1.80 ± 0.28
Zn	10.4 ± 3.89	51.8 ± 2.62	172 ± 2.00	180 ± 0.00	3327 ± 141	18.2 ± 0.28	36.1 ± 1.91	162 ± 1.27

[a] NA = not available because the extracted concentrations were below the particular detection limits.

mixing curve, so the Pb in these soils must come from sources with higher $^{206}Pb/^{207}Pb$ ratios and Pb concentrations than the local geochemical background of ~17 mg/kg. The most likely source of Pb to these soils is construction waste, which according to the literature contains highly variable, but generally higher concentrations of Pb (Balali et al., 2023; Butera et al., 2014; Chen and Zhou, 2020) than the local background. Unfortunately, to the best of our knowledge, data on the Pb isotopic composition of construction materials are not available. However, it is likely that some types of materials, such as bricks, concrete, mortar and tiles, could have higher $^{206}Pb/^{207}Pb$ ratios because they contain minerals of natural origin. Common minerals in construction waste materials that contain Pb are feldspars, phyllosilicates (illite/muscovite and chlorite) and calcite (Bianchini et al., 2005; Rodrigues et al., 2013).

3.3. Geochemical fractionation and mineralogy

Geochemical fractionation of metal (loid)s based on the BCR sequential extraction before bioaccessibility testing is shown in Fig. 6. The percentages of metal (loid)s (mean ± standard deviation) in the exchangeable/carbonate fraction (EC1) followed the order: Cd (63.4 ± 11.6%) ≫ Zn (27.0 ± 12.1%) > Pb(20.7 ± 7.79%) ≈ Cu(18.9 ± 7.86%) > Sn (11.5 ± 2.45%) ≈ Mn (11.1 ± 3.82%) ≈ As (9.48 ± 5.50%) ≈ Ni (9.30 ± 4.29%) > Co(4.82 ± 1.87%) > Cr (2.73 ± 0.47%) > V (1.62 ± 1.15%) ≈ Fe (1.51 ± 0.63%) ≈ Sb(1.06 ± 2.23%). More than one third of the *aqua regia* As, Mn, Pb and Sb concentrations was in the reducible fraction (RED2). The RED2 fraction was also a significant reservoir of other metals (>20%, excepting Cr and Sn). Generally, the contribution of oxidisable fraction (OX3) to the metal (loid) concentrations was lower, excepting Cu (27.8 ± 8.00%). Chromium, V, Sn, Fe, Co, Sb, Ni and As dominated in the residual fraction (RES4) with contributions of 83.3 ± 6.31%, 65.8 ± 8.69%, 65.2 ± 9.73%, 64.4 ± 7.77%, 63.7 ± 10.2%, 63.6 ± 10.6%, 55.9 ± 7.48% and 49.3 ± 12.8%, respectively.

Of the crystalline phases, quartz (SiO_2; 9–60 wt%) and calcite ($CaCO_3$; 2–11 wt%) were common and most abundant in all five characterised soils (Figs. S3 and S4). Other crystalline phases were also abundant but not in each soil. For example, hematite (Fe_2O_3) had a high proportion in MSWI ash–soil mixtures, B13a, b (up to 18 wt%), but it was not identified using XRD analysis in the other soils. Amorphous phases contributed a significant proportion to soils (27–63 wt%) and consisted of glasses, Fe (hydr)oxides and carbonaceous material (Fig. 7). Green and blue grains in soil–MSWI ash mixtures (Fig. S3) were identified as malachite ($Cu_2CO_3(OH)_2$)/brochantite ($Cu_4(SO_4)(OH)_6$) and lazurite ($Na_7Ca(Al_6Si_6O_{24})(SO_4)(S_3) \times H_2O$), respectively. Almost all grains subjected to EMP analyses contained several metal (loid)s (Table 2), which is particularly significant in relation to phases soluble in the acidic stomach environment, such as Ca-carbonates and amorphous Fe (hydr)oxides, and thus to the degree of metal (loid) bioaccessibility (Smith et al., 2011). The main elements present in the glasses, i.e., Si, Al, Fe and Ca were in accordance with the literature (Bayuseno and Schmahl, 2010; Izquierdo et al., 2002; Wei et al., 2011). Trace metal (loid)s were randomly distributed within the respective component, with no preference for a particular phase, which may complicate the environmental and health risk predictions. For example, the mean concentration of Cu, Pb, Zn and As was 0.09 ± 0.15, 0.20 ± 0.35, 0.84 ± 0.89 and 0.05 ± 0.46 wt% in Fe (hydr)oxides, while the glass particles contained 0.07 ± 0.13, 0.68 ± 3.42, 0.45 ± 1.20 and 0.14 ± 0.25 wt%, respectively. Occasionally, metal-enriched grains were observed, e.g., Sn-rich grain (up to 34.5 wt% SnO), Zn (up to ~18 wt% ZnO) or Pb (19.1 wt% PbO). Calcites, either as individual grains or coatings, entrapped mostly Cu, Ni, Pb, Sn and Zn (Fig. 7, S5; Table 2), which was also reflected in their relatively high occurrence in the EC1 fraction (see paragraph above).
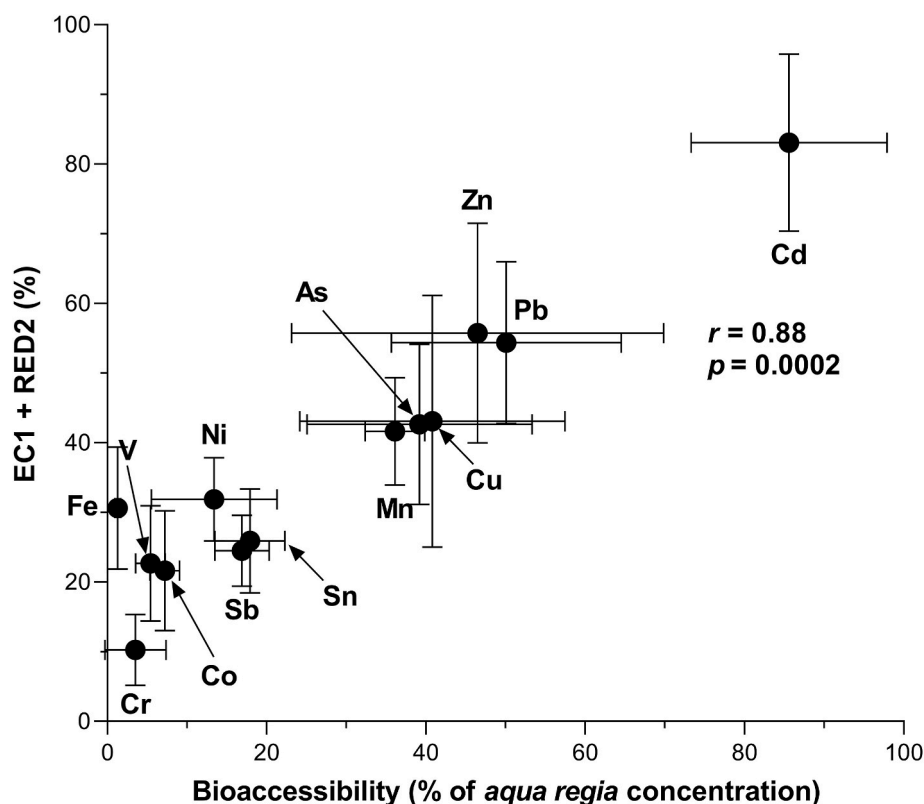

Fig. 8. Correlation of oral bioaccessibility (gastric phase) of metal (loid)s averaged over all 8 soils with the sum of exchangeable/carbonate (EC1) and reducible (RED2) fractions. Error bars represent standard deviation ($n = 16$).
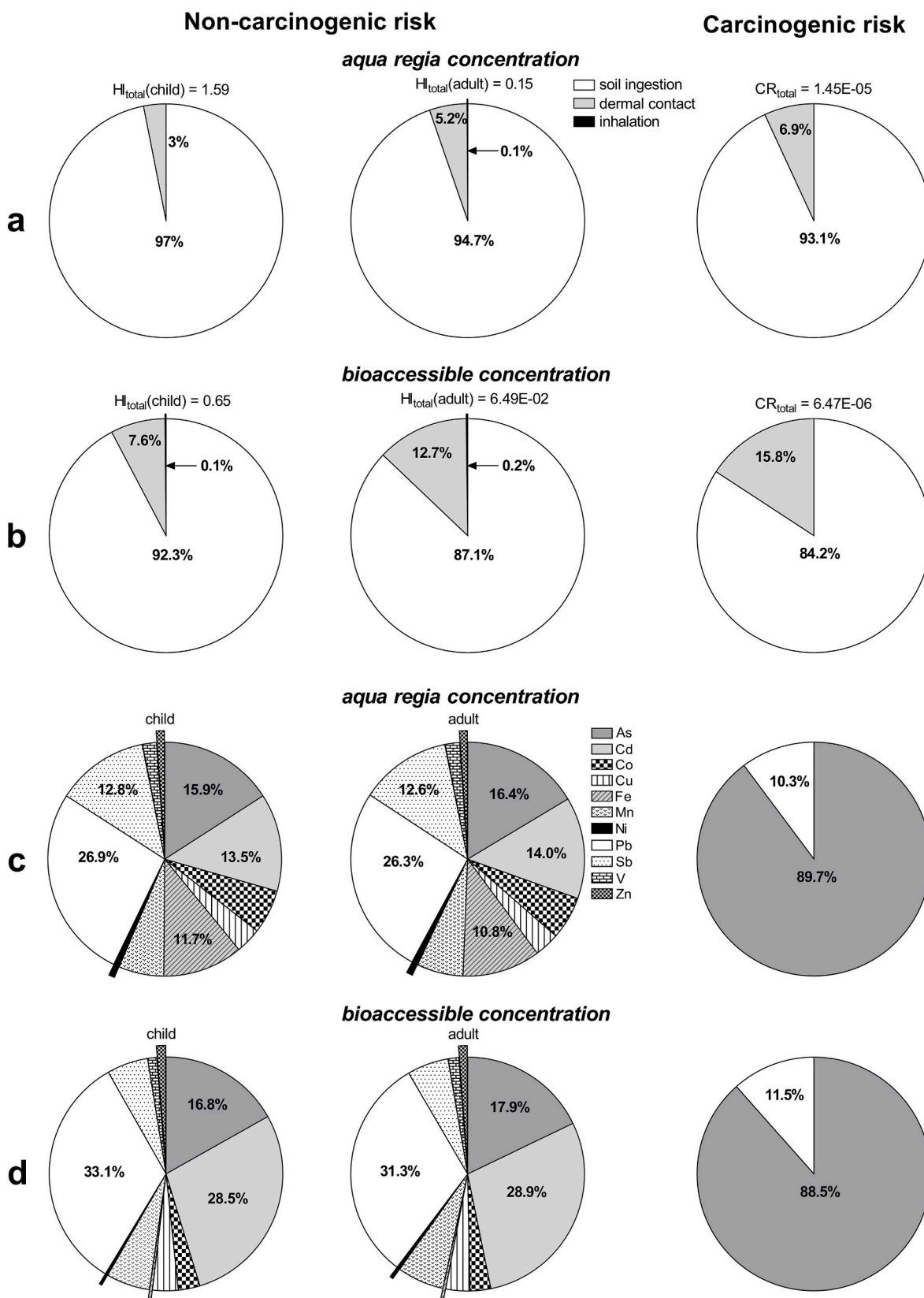
Fig. 9. Contributions of exposure routes to the total non-carcinogenic (HI$_{total}$) and carcinogenic risk (CR$_{total}$) estimated from *aqua regia* and bioaccessible concentrations (rows **a** and **b**, respectively), and contributions of individual metal (loid)s to HI$_{total}$ and CR$_{total}$ where row **c** = estimate from *aqua regia* concentrations and row **d** = estimate from bioaccessible concentrations. Chromium and tin do not appear because their contribution was less than 0.05%. Metal (loid) contributions higher than 10% are only shown in figures.

3.4. Bioaccessibility and its relationship to fractionation and mineralogy

Significant differences in bioaccessibility were observed among the tested soils and metal (loid)s (Table 3). Bioaccessible concentrations of all metal (loid)s were positively correlated with their *aqua regia* concentrations ($p < 0.01$) and bioaccessible fractions followed the order: Cd (85.6 ± 12.3%) > Pb(50.1 ± 14.4%) ≈ Zn (46.5 ± 23.4%) > Cu(40.8 ± 16.7%) ≈ As (39.2 ± 14.1%) > Mn (36.1 ± 3.67%) > Sn(17.9 ± 4.39%) ≈ Sb(16.9 ± 3.39%) > Ni(13.4 ± 7.88%) > Co(7.17 ± 1.84%) > V (5.41 ± 1.85%) ≈ Cr (3.50 ± 3.85%) > Fe (1.30 ± 0.36%). This trend was consistent with decreasing metal (loid) percentages in EC1 and RED2 fractions (Fig. 8). Generally, the highest bioaccessibility of metal (loid)s, except for Sb, exhibited the sample B13a from the MSWI ash outcrop (Table 3). Compared to other samples, the sample B13a was the most abundant in calcite (~11 wt%) and Fe (hydr)oxides (Fig. S3). These mineral phases are readily attacked by acidified glycine, thus releasing the incorporated/adsorbed metal (loid)s (Smith et al., 2008; Xie et al., 2023; Xu and Fu, 2022). Furthermore, the percentages of metal (loid)s in EC1 and RED2 fractions of the sample B13a were highest among the soils. On the other hand, this sample was rich in Si-based glasses, containing non-negligible concentrations of metal (loid)s but due to their limited solubility (Mantovani et al., 2023), they were unlikely to contribute much to bioaccessible metal (loid)s. However, Ettler et al. (2019) demonstrated the etching of glasses with an acidic solution of glycine. The bioaccessibility of As, Mn, Ni, Pb, Sn and Zn correlated positively with the sum of EC1+RED2, and Cd with EC1 (Fig. S6). Correlations of metal (loid) bioaccessibility with their EC1 and RED2 fractions were documented in several studies (Ai et al., 2019; Chu et al., 2022; Ding et al., 2022; Li et al., 2022; Pelfrêne et al., 2011; Wu et al., 2024) and explained by the fact that the orally bioaccessible metal (loid)s originated primarily from their acid-soluble and Fe-oxide-bound fractions in soil. To understand the fractionation changes of metal (loid)s during bioaccessibility testing, samples B6 and B13a were subjected to BCR sequential extraction after bioaccessibility test (Fig. 6). In terms of EC1, this fraction was largely depleted for almost all metal (loid)s, consistent with the finding that calcite almost completely disappeared after glycine extraction (Ettler et al., 2019). Although only a limited number of samples from those tested for bioaccessibility were mineralogically studied, the calcite content, as a chemically readily reactive mineral with an acidified glycine solution, had an effect on the bioaccessibility of Cd, Cu, Pb and Sn in the sense that samples with a higher calcite content (B6 and B13a) had a higher bioaccessibility of these four metals than soils B10 and B16 with a lower calcite content (Table 3). Several studies showed that the gastric bioaccessibility of trace metal (loid)s in urban soils positively depended on the $CaCO_3$ content, which is probably related to the easy mobilisation of carbonate bound metal (loid)s at low pH of the gastric environment (De Miguel et al., 2012; Hiller et al., 2022; Izquierdo et al., 2015). A significant decrease of several metal (loid)s, e.g., As, Cu, Fe, Mn, Pb, Sn and Zn, also occurred in the RED2 fraction, with the RES4 fraction contributing more to the total metal (loid) concentration, while the oxidisable fraction remained mostly unchanged (Fig. 6). Smith et al. (2008, 2011) showed on the basis of XANES measurements and sequential extractions that Fe (hydr)oxides were one of the sources of bioaccessible Pb and As during the gastric phase, respectively.

3.5. Human health risk assessment

When *aqua regia* metal (loid) concentrations were taken into account, i.e., relative bioavailability (RBA) = 1, the value of HI_{total} for children reached 1.59, indicating the existence of a non-carcinogenic risk in the area (Fig. 9). However, after adjusting to bioaccessible fractions, the HI_{total} value was more than halved to 0.65. On the other hand, no non-carcinogenic risk was found for adults, even assuming RBA = 1. In any case, soil ingestion was primary contributor to HI_{total} (Fig. 9) and driven by the characteristic non-essential metal (loid)s, Pb, As, Cd and

Sb. Iron, as essential but also toxic metal (Brewer, 2010), also considerably contributed to HI_{total} due to its high *aqua regia* concentrations in soils, however, because of very low Fe bioaccessibility (1.30 ± 0.36%), its contribution to the total non-carcinogenic risk was very small (lower than 0.5%) after correcting for bioaccessibility (Fig. 9). Dermal contact was a minor contributor to non-carcinogenic risks, while the inhalation was negligible, which agreed with previous studies (Antoniadis et al., 2019; Obiri-Nyarko et al., 2021). Lead, the largest contributor to HI_{total}, is a neurotoxic and bio-accumulative metal that causes cognitive and neuro-behavioural impairments, especially in children (Dong et al., 2020; Mielke et al., 2019; Pavilonis et al., 2022). With long-term exposure to soil Pb at concentrations of hundreds mg/kg, the blood lead levels can reach a threshold of 5.0 µg/dL (Bradham et al., 2017; Wu et al., 2020), above which the likelihood of cognitive and behavioural impairment in children increases (Kuraeiad and Kotepui, 2021; Maidoumi et al., 2022).

The total carcinogenic risk (CR_{total}) based on the *aqua regia* concentrations with a value of 1.45×10^{-5} was in the acceptable range of 10^{-4}–10^{-6}. Refinement of the carcinogenic risk using bioaccessible concentrations resulted in a significant decrease of CR_{total} by 47% to a value of 6.47×10^{-6}, which was within the acceptable cancer risk. As in the case of non-carcinogenic risk, the carcinogenic risk was contributed almost exclusively by soil ingestion and the rest by dermal absorption (Fig. 9). Arsenic had the largest contribution to the total carcinogenic risk (up to 90%). This result is consistent with other studies (Du and Li, 2023; Obiri-Nyarko et al., 2021) and relates to the fact that As is confirmed carcinogen to humans belonging to Group 1 according to International Agency for Research on Cancer (IARC, 2004).

4. Conclusions

This study showed that the concentrations of metal (loid)s in the soils of the historical landfill fluctuated considerably, both spatially and vertically. *Aqua regia* concentrations of Cd, Cu, Pb, Sb, Sn and Zn in landfill soils varied by up to three orders of magnitude. More than 10% of soils were categorised as heavily to extremely contaminated with Cd, Cu, Pb, Sb, Sn and Zn according to I_{geo} values, while metals such as Co, Cr, Fe, Mn, Ni and V in most soils showed moderate soil contamination. Gastric bioaccessibility varied among the soils and metal (loid)s, and in some cases, correlated with the first two steps of the BCR sequential extraction. While Cr, Co, Fe, Ni, Sb, Sn and V were mainly in the residual fraction, significant amounts of As, Cd, Cu, Pb and Zn were found in the available fraction. The weathered MSWI ash was found to be the most geochemically labile in an acidic environment, likely due to the alkaline nature and mineralogy dominated by amorphous Fe (hydr)oxides, calcite and other solid phases. Based on the results of multivariate statistical methods, determination of the degree of contamination of landfill soils by individual metal (loid)s, comparison with local background concentrations and interpretation of Pb isotope ratios ($^{206}Pb/^{207}Pb$ and $^{208}Pb/^{206}Pb$), it could be assumed that Cd, Cu, Pb, Sb, Sn and Zn had a predominant anthropogenic origin with significant contribution from MSWI ash as their source material. Other metals, especially Co, Cr, Fe, Mn, Ni and V were primarily of lithogenic origin with rarely elevated concentrations. In summary, these data documented significant variability in the geochemical properties of landfill soils, even over a relatively small area. The landfill is being considered as a residential/recreational zone in the near future, but as the results document, remediation would be appropriate, regardless of the fact that human health risks from soil exposure after accounting for bioaccessibility were not demonstrated.

CRediT authorship contribution statement

Edgar Hiller: Writing – review & editing, Writing – original draft, Supervision, Resources, Methodology, Investigation, Data curation, Conceptualization. **Tomáš Faragó:** Visualization, Methodology, Investigation. **Martin Kolesár:** Visualization, Investigation, Funding acquisition. **Lenka Filová:** Writing – review & editing, Visualization, Software, Formal analysis. **Martin Mihaljevič:** Writing – review & editing, Validation, Project administration, Investigation. **Ľubomír Jurkovič:** Visualization, Supervision, Project administration, Funding acquisition. **Rastislav Demko:** Validation, Investigation. **Andrej Machlica:** Resources, Investigation. **Ján Štefánek:** Visualization, Resources, Investigation. **Martina Vítková:** Writing – review & editing, Investigation.

Declaration of competing interest

The authors declare that they have no known competing financial interests or personal relationships that could have appeared to influence the work reported in this paper.

Data availability

Data will be made available on request.

Acknowledgements

Appendix A. Supplementary data

Supplementary data to this article can be found online at https://doi.org/10.1016/j.chemosphere.2024.142677.

References

Adamcová, D., Vaverková, M.D., Bartoň, S., Havlíček, Z., Broušková, E., 2016. Soil contamination in landfills: a case study of a landfill in Czech Republic. Solid Earth 7, 239–247. https://doi.org/10.5194/se-7-239-2016.

Adelopo, A.O., Haris, P.I., Alo, B.I., Huddersman, K., Jenkins, R.O., 2018. Multivariate analysis of the effects of age, particle size and landfill depth on heavy metals pollution content of closed and active landfill precursors. Waste Manage. (Tucson, Ariz.) 78, 227–237. https://doi.org/10.1016/j.wasman.2018.05.040.

Adewumi, A.J., Ogundele, O.D., 2024. Hidden hazards in urban soils: a meta-analysis review of global heavy metal contamination (2010-2022), sources and its ecological and health consequences. Sustain. Environ. 10, 2293239 https://doi.org/10.1080/27658511.2023.2293239.

Ahmad, W., Zubair, M., Ahmed, M., Ahmad, M., Latif, S., Hameed, A., Kanwal, Q., Iqbal, D.N., 2023. Assessment of potentially toxic metal(loid)s contamination in soil near the industrial landfill and impact on human health: an evaluation of risk. Environ. Geochem. Health 45, 4353–4369. https://doi.org/10.1007/s10653-023-01499-7.

Ai, Y., Li, X., Gao, Y., Zhang, M., Zhang, Y., Zhang, X., Yan, X., Liu, B., Yu, H., 2019. In vitro bioaccessibility of potentially toxic metals (PTMs) in Baoji urban soil (NW China) from different functional areas and its implication for health risk assessment. Environ. Geochem. Health 41, 1055–1073. https://doi.org/10.1007/s10653-018-0197-6.

Akoto, O., Nimako, C., Asante, J., Bailey, D., 2016. Heavy metals enrichment in surface soil from abandoned waste disposal sites in a hot and wet tropical area. Environ. Process. 3, 747–761. https://doi.org/10.1007/s40710-016-0183-x.

Alghamdi, A.G., Aly, A.A., Ibrahim, H.M., 2021. Assessing the environmental impacts of municipal solid waste landfill leachate on groundwater and soil contamination in western Saudi Arabia. Arabian J. Geosci. 14, 350. https://doi.org/10.1007/s12517-021-06583-9.

Alloway, B.J., 2013. Sources of heavy metals and metalloids in soils. In: Alloway, B.J. (Ed.), Heavy Metals in Soils. Springer, Dordrecht, pp. 11–50.

Anonymous, 2002. Land atlas of the Slovak republic, first ed. The Slovak environmental agency (SEA). Banská Bystrica. Slovakia, p. 344.

Antoniadis, V., Shaheen, S.M., Levizou, E., Shahid, M., Niazi, N.K., Vithanage, M., Oki, Y. S., Bolan, N., Rinklebe, J., 2019. A critical prospective analysis of the potential toxicity of trace element regulation limits in soils worldwide: are they protective concerning health risk assessment? – a review. Environ. Int. 127, 819–847. https://doi.org/10.1016/j.envint.2019.03.039.

Balali, A., Gholami, S., Javanmardi, M., Valipour, A., Yunusa-Kaltungo, A., 2023. Assessment of heavy metal pollution in the soil of a construction and demolition waste landfill. Environ. Nanotechnol. Monit. Manag. 20, 100856 https://doi.org/10.1016/j.enmm.2023.100856.

Barbieri, M., Sappa, G., Vitale, S., Parisse, B., Battistel, M., 2014. Soil control of trace metals concentrations in landfills: a case study of the largest landfill in Europe, Malagrotta, Rome. J. Geochem. Explor. 143, 146–154. https://doi.org/10.1016/j.gexplo.2014.04.001.

Bayuseno, A.P., Schmahl, W.W., 2010. Understanding the chemical and mineralogical properties of the inorganic portion of MSWI bottom ash. Waste Manage. (Tucson, Ariz.) 30, 1509–1520. https://doi.org/10.1016/j.wasman.2010.03.010.

Bianchini, G., Marrocchino, E., Tassinari, R., Vaccaro, C., 2005. Recycling of construction and demolition waste materials: a chemical–mineralogical appraisal. Waste Manage. (Tucson, Ariz.) 25, 149–159. https://doi.org/10.1016/j.wasman.2004.09.005.

Billmann, M., Hulot, C., Pauget, B., Badreddine, R., Papin, A., Pelfrêne, A., 2023. Oral bioaccessibility of PTEs in soils: a review of data, influencing factors and application in human health risk assessment. Sci. Total Environ. 896, 165263 https://doi.org/10.1016/j.scitotenv.2023.165263.

Binner, H., Sullivan, T., Jansen, M.A.K., McNamara, M.E., 2023. Metals in urban soils of Europe: a systematic review. Sci. Total Environ. 854, 158734 https://doi.org/10.1016/j.scitotenv.2022.158734.

Bolan, N., Kumar, M., Singh, E., Kumar, A., Singh, L., Kumar, S., Keerthanan, S., Hoang, S.A., El-Naggar, A., Vithanage, M., Sarkar, B., Wijesekara, H., Diyabalanage, S., Sooriyakumar, P., Vinu, A., Wang, H., Kirkham, M.B., Shaheen, S. M., Rinklebe, J., Siddique, K.H.M., 2022. Antimony contamination and its risk management in complex environmental settings: a review. Environ. Int. 158, 106908 https://doi.org/10.1016/j.envint.2021.106908.

Botsou, F., Sungur, A., Kelepertzis, E., Kypritidou, Z., Daferera, O., Massas, I., Argyraki, A., Skordas, K., Soylak, M., 2022. Estimating remobilization of potentially toxic elements in soil and road dust of an industrialized urban environment. Environ. Monit. Assess. 194, 526. https://doi.org/10.1007/s10661-022-10200-x.

Bradham, K.D., Nelson, C.M., Kelly, J., Pomales, A., Scruton, K., Dignam, T., Misenheimer, J.C., Li, K., Obenour, D.R., Thomas, D.J., 2017. Relationship between total and bioaccessible lead on children's blood lead levels in urban residential Philadelphia soils. Environ. Sci. Technol. 51, 10005–10011. https://doi.org/10.1021/acs.est.7b02058.

Brewer, G.J., 2010. Risks of copper and iron toxicity during aging in humans. Chem. Res. Toxicol. 23, 319–326. https://doi.org/10.1021/tx900338d.

Butera, S., Christensen, T.H., Astrup, T.F., 2014. Composition and leaching of construction and demolition waste: inorganic elements and organic compounds. J. Hazard Mater. 276, 302–311. https://doi.org/10.1016/j.jhazmat.2014.05.033.

Chen, Y., Zhou, Y., 2020. The contents and release behavior of heavy metals in construction and demolition waste used in freeway construction. Environ. Sci. Pollut. Res. 27, 1078–1086. https://doi.org/10.1007/s11356-019-07067-w.

Chu, Z., Lin, C., Yang, K., Cheng, H., Gu, X., Wang, B., Wu, L., Ma, J., 2022. Lability, bioaccessibility, and ecological and health risks of anthropogenic toxic heavy metals in the arid calcareous soil around a nonferrous metal smelting area. Chemosphere 307, 136200. https://doi.org/10.1016/j.chemosphere.2022.136200.

Claes, H., Cappuyns, V., Swennen, R., Meyer, R., Seemann, T., Stanjek, H., Sindern, S., Tock, P., 2023. Importance of arsenic bioaccessibility in health risk assessment based on iron "Minette" rocks and related soils. Ecotoxicol. Environ. Saf. 266, 115567 https://doi.org/10.1016/j.ecoenv.2023.115567.

Critto, A., Carlon, C., Marcomini, A., 2003. Characterization of contaminated soil and groundwater surrounding an illegal landfill (S. Giuliano, Venice, Italy) by principal component analysis and kriging. Environ. Pollut. 122, 235–244. https://doi.org/10.1016/S0269-7491(02)00296-8.

de Souza, V.B., Hollas, C.E., Bortoli, M., Manosso, F.C., de Souza, D.Z., 2023. Heavy metal contamination in soils of a decommissioned landfill southern Brazil: ecological and health risk assessment. Chemosphere 339, 139689. https://doi.org/10.1016/j.chemosphere.2023.139689.

De Miguel, E., Mingot, J., Chacón, E., Charlesworth, S., 2012. The relationship between soil geochemistry and the bioaccessibility of trace elements in playground soil. Environ. Geochem. Health 34, 677–687. https://doi.org/10.1007/s10653-012-9486-7.

Ding, S., Guan, D.X., Dai, Z.H., Su, J., Teng, H.H., Ji, J., Liu, Y., Yang, Z., Ma, L.Q., 2022. Nickel bioaccessibility in soils with high geochemical background and anthropogenic contamination. Environ. Pollut. 310, 119914 https://doi.org/10.1016/j.envpol.2022.119914.

Dodd, M., Amponsah, L.O., Grundy, S., Darko, G., 2023. Human health risk associated with metal exposure at Agbogbloshie e-waste site and the surrounding neighbourhood in Accra, Ghana. Environ. Geochem. Health 45, 4515–4531. https://doi.org/10.1007/s10653-023-01503-0.

Dodd, M., Lee, D., Nelson, J., Verenitch, S., Wilson, R., 2024. In vitro bioaccessibility round robin testing for arsenic and lead in standard reference materials and soil samples. Integrated Environ. Assess. Manag. https://doi.org/10.1002/ieam.4891.

Dong, C., Taylor, M.P., Gulson, B., 2020. A 25-year record of childhood blood lead exposure and its relationship to environmental sources. Environ. Res. 186, 109357 https://doi.org/10.1016/j.envres.2020.109357.

Drahota, P., Raus, K., Rychlíková, E., Rohovec, J., 2018. Bioaccessibility of As, Cu, Pb, and Zn in mine waste, urban soil, and road dust in the historical mining village of Kaňk, Czech Republic. Environ. Geochem. Health 40, 1495–1512. https://doi.org/10.1007/s10653-017-9999-1.

Du, C., Li, Z., 2023. Contamination and health risks of heavy metals in the soil of a historical landfill in northern China. Chemosphere 313, 137349. https://doi.org/10.1016/j.chemosphere.2022.137349.

Elnabi, M.K.A., Elkaliny, N.E., Elyazied, M.M., Azab, S.H., Elkhalifa, S.A., Elmasry, S., Mouhamed, M.S., Shalamesh, E.M., Alhorieny, N.A., Elaty, A.E.A., Elgendy, I.M., Etman, A.E., Saad, K.E., Tsigkou, K., Ali, S.S., Kornaros, M., Mahmoud, Y.A.-G., 2023. Toxicity of heavy metals and recent advances in their removal: a review. Toxics 11, 580. https://doi.org/10.3390/toxics11070580.

Ettler, V., Mihaljevič, M., Komárek, M., 2004. ICP-MS measurements of lead isotopic ratios in soils heavily contaminated by lead smelting: tracing the sources of pollution. Anal. Bioanal. Chem. 378, 311–317. https://doi.org/10.1007/s00216-003-2229-y.

Ettler, V., Cíhlová, M., Jarošíková, A., Mihaljevič, M., Drahota, P., Křibek, B., Vaněk, A., Penížek, V., Sracek, O., Klementová, M., Engel, Z., Kamona, F., Mapani, B., 2019. Oral bioaccessibility of metal(loid)s in dust materials from mining areas of northern Namibia. Environ. Int. 124, 205–215. https://doi.org/10.1016/j.envint.2018.12.027.

Ettler, V., Raus, K., Mihaljevič, M., Křibek, B., Vaněk, A., Penížek, V., Sracek, O., Koubová, M., Mapani, B., 2023. Bioaccessible metals in dust materials from non-sulfide Zn deposit and related hydrometallurgical operation. Chemosphere 345, 140498. https://doi.org/10.1016/j.chemosphere.2023.140498.

Gujre, N., Mitra, S., Soni, A., Agnihotri, R., Rangan, L., Rene, E.R., Sharma, M.P., 2021. Speciation, contamination, ecological and human health risks assessment of heavy metals in soils dumped with municipal solid wastes. Chemosphere 262, 128013. https://doi.org/10.1016/j.chemosphere.2020.128013.

Gworek, B., Dmuchowski, W., Koda, E., Marecka, M., Baczewska, A.H., Brągoszewska, P., Sieczka, A., Osiński, P., 2016. Impact of the municipal solid waste Łubna landfill on environmental pollution by heavy metals. Water 8, 470. https://doi.org/10.3390/w8100470.

Haack, U.K., Heinrichs, H., Gutsche, F.H., Plessow, K., 2003. The isotopic composition of anthropogenic Pb in soil profiles of Northern Germany: evidence for pollutant Pb from a continent-wide mixing system. Water Air Soil Pollut. 150, 113–134. https://doi.org/10.1023/A:1026142501593.

Hamelin, B., Ferrand, J.L., Alleman, L., Nicolas, E., Veron, A., 1997. Isotopic evidence of pollutant lead transport from North America to the subtropical North Atlantic gyre. Geochim. Cosmochim. Acta. 61, 4423–4428. https://doi.org/10.1016/S0016-7037(97)00242-1.

Hansmann, W., Köppel, V., 2000. Lead-isotopes as tracers of pollutants in soils. Chem. Geol. 171, 123–144. https://doi.org/10.1016/S0009-2541(00)00230-8.

Helser, J., Vassilieva, E., Cappuyns, V., 2022. Environmental and human health risk assessment of sulfidic mine waste: bioaccessibility, leaching and mineralogy. J. Hazard Mater. 424 (Part A), 127313 https://doi.org/10.1016/j.jhazmat.2021.127313.

Hiller, E., Mihaljevič, M., Filová, L., Lachká, L., Jurkovič, Ľ., Kulikova, T., Fajčíková, K., Šimurková, M., Tatarková, V., 2017. Occurrence of selected trace metals and their oral bioaccessibility in urban soils of kindergartens and parks in Bratislava (Slovak Republic) as evaluated by simple in vitro digestion procedure. Ecotoxicol. Environ. Saf. 144, 611–621. https://doi.org/10.1016/j.ecoenv.2017.06.040.

Hiller, E., Pilková, Z., Filová, L., Jurkovič, Ľ., Mihaljevič, M., Lacina, P., 2021. Concentrations of selected trace elements in surface soils near crossroads in the city of Bratislava (the Slovak Republic). Environ. Sci. Pollut. Res. 28, 5455–5471. https://doi.org/10.1007/s11356-020-10822-z.

Hiller, E., Pilková, Z., Filová, L., Mihaljevič, M., Špirová, V., Jurkovič, Ľ., 2022. Metal (loid) concentrations, bioaccessibility and stable lead isotopes in soils and vegetables from urban community gardens. Chemosphere 305, 135499. https://doi.org/10.1016/j.chemosphere.2022.135499.

Hölzle, I., 2019. Contaminant patterns in soils from landfill mining. Waste Manage. (Tucson, Ariz.) 83, 151–160. https://doi.org/10.1016/j.wasman.2018.11.013.

Hölzle, I., Somani, M., Ramana, G.V., Datta, M., 2022. Heavy metals in soil-like material from landfills – resource or contaminants? J. Clean. Prod. 369, 133136 https://doi.org/10.1016/j.jclepro.2022.133136.

Hussein, M., Yoneda, K., Mohd-Zaki, Z., Amir, A., Othman, N., 2021. Heavy metals in leachate, impacted soils and natural soils of different landfills in Malaysia: an alarming threat. Chemosphere 267, 128874. https://doi.org/10.1016/j.chemosphere.2020.128874.

IARC, 2004. IARC Monographs on the Evaluation of Carcinogenic Risks to Humans, Volume 84, Some Drinking-Water Disinfectants and Contaminants, Including Arsenic. International Agency for Research on Cancer, Lyon, France.

Ihedioha, J.N., Ukoha, P.O., Ekere, N.R., 2017. Ecological and human health risk assessment of heavy metal contamination in soil of a municipal solid waste dump in Uyo, Nigeria. Environ. Geochem. Health 39, 497–515. https://doi.org/10.1007/s10653-016-9830-4.

ISO, 2020. ISO 54321:2020 Soil, treated biowaste, sludge and waste — Digestion of aqua regia soluble fractions of elements. The International Organization for Standardization.

Izquierdo, M., De Miguel, E., Ortega, M.F., Mingot, J., 2015. Bioaccessibility of metals and human health risk assessment in community urban gardens. Chemosphere 135, 312–318. https://doi.org/10.1016/j.chemosphere.2015.04.079.

Izquierdo, M., López-Soler, Á., Ramonich, E.V., Barra, M., Querol, X., 2002. Characterisation of bottom ash from municipal solid waste incineration in Catalonia. Chem. Technol. Biotechnol. 77, 576–583. https://doi.org/10.1002/jctb.605.

Kabata-Pendias, A., Mukherjee, A.B., 2007. Trace Elements from Soil to Human, first ed. Springer-Verlag, Berlin, p. 550.

Karimian, S., Shekoohiyan, S., Moussavi, G., 2021. Health and ecological risk assessment and simulation of heavy metal-contaminated soil of Tehran landfill. RSC Adv. 11, 8080–8095. https://doi.org/10.1039/d0ra08833a.

Kelepertzis, E., Argyraki, A., 2015. Geochemical associations for evaluating the availability of potentially harmful elements in urban soils: lessons learnt from Athens, Greece. Appl. Geochem. 59, 63–73. https://doi.org/10.1016/j.apgeochem.2015.03.019.

Khan, M.A., Nawab, J., Khan, A., Brusseau, M.L., Khan, S.N., Ali, N., Bahadur, S., Khan, S., Huang, Q., 2023. Human health and ecological risks associated with total and bioaccessible concentrations of cadmium and lead in urban park soils. Bull. Environ. Contam. Toxicol. 110, 61. https://doi.org/10.1007/s00128-023-03703-x.

Kierulf, A., Ollson, C., Whitehead, C., Beauchemin, D., Koch, I., 2022. Literature review and meta-analysis of gastric and intestinal bioaccessibility for nine inorganic elements in soils and soil-like media for use in human health risk assessment. Int. J. Hyg Environ. Health 240, 113929. https://doi.org/10.1016/j.ijheh.2022.113929.

Kumar, D., Malik, S., Rani, R., Kumar, R., Duhan, J.S., 2023. Behavior, risk, and bioremediation potential of heavy metals/metalloids in the soil system. Rend. Lincei-Sci. Fis. 34, 809–831. https://doi.org/10.1007/s12210-023-01166-0.

Kuraeiad, S., Kotepui, M., 2021. Blood lead level and renal impairment among adults: a meta-analysis. Int. J. Environ. Res. Publ. Health 18, 4174. https://doi.org/10.3390/ijerph18084174.

Kyene, M.O., Gbeddy, G., Mensah, T., Acheampong, C., Kumi-Amoah, G., Ketemepi, H.K., Brimah, A.K., Akyea-Larbi, K., Darko, D.A., 2023. Bioaccessibility and children health risk assessment of soil-laden heavy metals from school playground and public parks in Accra, Ghana. Environ. Monit. Assess. 195, 1199. https://doi.org/10.1007/s10661-023-11818-1.

Kynčlová, P., Hron, K., Filzmoser, P., 2017. Correlation between compositional parts based on symmetric balances. Math. Geosci. 49, 777–796. https://doi.org/10.1007/s11004-016-9669-3.

Li, S.W., Sun, H.J., Li, H.B., Luo, J., Ma, L.Q., 2016. Assessment of cadmium bioaccessibility to predict its bioavailability in contaminated soils. Environ. Int. 94, 600–606. https://doi.org/10.1016/j.envint.2016.06.022.

Li, H.B., Li, M.Y., Zhao, D., Li, J., Li, S.W., Xiang, P., Juhasz, A.L., Ma, L.Q., 2020. Arsenic, lead, and cadmium bioaccessibility in contaminated soils: measurements and validations. Crit. Rev. Environ. Sci. Technol. 50, 1303–1338. https://doi.org/10.1080/10643389.2019.1656512.

Li, S.W., Chang, M.H., Huang, X.Y., Li, H.L., Li, H.B., Ma, L.Q., 2022. Coupling in vitro assays with sequential extraction to investigate cadmium bioaccessibility in contaminated soils. Chemosphere 288, 132655. https://doi.org/10.1016/j.chemosphere.2021.132655.

Liang, J.H., Lin, X.Y., Huang, D.K., Xue, R.Y., Fu, X.Q., Ma, L.Q., Li, H.B., 2022. Nickel oral bioavailability in contaminated soils using a mouse urinary excretion bioassay: variation with bioaccessibility. Sci. Total Environ. 839, 156366 https://doi.org/10.1016/j.scitotenv.2022.156366.

Lu, X., Yang, Q., Wang, H., Zhu, Y., 2023. A global meta-analysis of the correlation between soil physicochemical properties and lead bioaccessibility. J. Hazard Mater. 453, 131440 https://doi.org/10.1016/j.jhazmat.2023.131440.

Luo, H., Cheng, Y., He, D., Yang, E.-H., 2019. Review of leaching behavior of municipal solid waste incineration (MSWI) ash. Sci. Total Environ. 668, 90–103. https://doi.org/10.1016/j.scitotenv.2019.03.004.

Maidoumi, S., Ouaziz, C.R., Ouisselsat, M., El Maouaki, A., Loukid, M., Lekouch, N., Pineau, A., Ahami, A., Sedki, A., 2022. Iron deficiency and cognitive impairment in children with low blood lead levels. Toxicol Rep 9, 1681–1690. https://doi.org/10.1016/j.toxrep.2022.08.008.

Mantovani, L., De Matteis, C., Tribaudino, M., Boschetti, T., Funari, V., Dinelli, E., Toller, S., Pelagatti, P., 2023. Grain size and mineralogical constraints on leaching in the bottom ashes from municipal solid waste incineration: a comparison of five plants in northern Italy. Front. Environ. Sci. 11, 1179272 https://doi.org/10.3389/fenvs.2023.1179272.

Mendoza, C.J., Garrido, R.T., Quilodran, R.C., Segovia, C.M., Parada, A.J., 2017. Evaluation of the bioaccessible gastric and intestinal fractions of heavy metals in contaminated soils by means of a simple bioaccessibility extraction test. Chemosphere 176, 81–88. https://doi.org/10.1016/j.chemosphere.2017.02.066.

Mielke, H.W., Gonzales, C.R., Powell, E.T., Egendorf, S.P., 2019. The concurrent decline of soil lead and children's blood lead in New Orleans. Proc. Natl. Acad. Sci. U. S. A. 116, 22058–22064. https://doi.org/10.1073/pnas.1906092116.

Mihaljevič, M., Ettler, V., Strnad, L., Šebek, O., Vonásek, F., Drahota, P., Rohovec, J., 2009. Isotopic composition of lead in Czech coals. Int. J. Coal Geol. 78, 38–46. https://doi.org/10.1016/j.coal.2008.09.018.

Mihaljevič, M., Ettler, V., Šebek, O., Sracek, O., Křibek, B., Kyncl, T., Majer, V., Veselovský, F., 2011. Lead isotopic and metallic pollution record in tree rings from the Copperbelt mining-smelting area, Zambia. Water Air Soil Pollut. 216, 657–668. https://doi.org/10.1007/s11270-010-0560-4.

Müller, G., 1979. Schwermetalle in den Sedimenten des Rheins - Veränderungen seit 1971. Umschau 79, 778–783.

Obiri-Nyarko, F., Duah, A.A., Karikari, A.Y., Agyekum, W.A., Manu, E., Tagoe, R., 2021. Assessment of heavy metal contamination in soils at the Kpone landfill site, Ghana:

implication for ecological and health risk assessment. Chemosphere 282, 131007. https://doi.org/10.1016/j.chemosphere.2021.131007.

Osibote, A., Oputu, O., 2020. Fate and partitioning of heavy metals in soils from landfill sites in Cape Town, South Africa: a health risk approach to data interpretation. Environ. Geochem. Health 42, 283–312. https://doi.org/10.1007/s10653-019-00348-w.

Oyelola, O.T., Babatunde, A.I., 2008. Effect of municipal solid waste on the levels of heavy metals in Olususun dumpsite soil, Lagos State, Nigeria. Int. J. Pure. Appl. Sci. 2, 17–21.

Pavilonis, B., Cheng, Z., Johnson, G., Maroko, A., 2022. Lead, soils, and children: an ecological analysis of lead contamination in parks and elevated blood lead levels in Brooklyn, New York. Arch. Environ. Contam. Toxicol. 82, 1–10. https://doi.org/10.1007/s00244-021-00902-7.

Pecina, V., Brtnický, M., Baltazár, T., Juřička, D., Kynický, J., Vašinová Galiová, M., 2021. Human health and ecological risk assessment of trace elements in urban soils of 101 cities in China: a meta-analysis. Chemosphere 267, 129215. https://doi.org/10.1016/j.chemosphere.2020.129215.

Pelfrène, A., Waterlot, C., Mazzuca, M., Nisse, C., Bidar, G., Douay, F., 2011. Assessing Cd, Pb, Zn human bioaccessibility in smelter-contaminated agricultural topsoils (northern France). Environ. Sci. Pollut. Res. 33, 477–493. https://doi.org/10.1007/s10653-010-9365-z.

Peña-Fernández, A., González-Muñoz, M.J., Lobo-Bedmar, M.C., 2014. Establishing the importance of human health risk assessment for metals and metalloids in urban environments. Environ. Int. 72, 176–185. https://doi.org/10.1016/j.envint.2014.04.007.

Prechthai, T., Parkpian, P., Visvanathan, C., 2008. Assessment of heavy metal contamination and its mobilization from municipal solid waste open dumping site. J. Hazard Mater. 156, 86–94. https://doi.org/10.1016/j.jhazmat.2007.11.119.

RAIS, 2023. The risk assessment information system (RAIS). U.S. Department of energy (DOE). Oak Ridge Operations Office (ORO) and Office of Environmental Management. https://rais.ornl.gov/.

Rauret, G., López-Sánchez, J.F., Sahuquillo, A., Rubio, R., Davidson, C., Ure, A., Quevauviller, Ph, 1999. Improvement of the BCR three step sequential extraction procedure prior to the certification of new sediment and soil reference materials. J. Environ. Monit. 1, 57–61. https://doi.org/10.1039/A807854H.

Reimann, C., Filzmoser, P., Hron, K., Kynčlová, P., Garrett, R.G., 2017. A new method for correlation analysis of compositional (environmental) data – a worked example. Sci. Total Environ. 607–608, 965–971. https://doi.org/10.1016/j.scitotenv.2017.06.063.

Rodrigues, F., Carvalho, M.T., Evangelista, L., de Brito, J., 2013. Physical–chemical and mineralogical characterization of fine aggregates from construction and demolition waste recycling plants. J. Clean. Prod. 52, 438–445. https://doi.org/10.1016/j.jclepro.2013.02.023.

Roy, A., Kumar, A., Bhattacharya, T., Biswas, J.K., Watts, M., 2024. Review: bioaccessibility of potentially harmful metals in dust and soil matrices. Expo. Health 16, 207–236. https://doi.org/10.1007/s12403-023-00546-z.

Silva-Gigante, M., Hinojosa-Reyes, L., Rosas-Castor, J.M., Quero-Jiménez, P.C., Pino-Sandoval, D.A., Guzmán-Mar, J.L., 2023. Heavy metals and metalloids accumulation in common beans (Phaseolus vulgaris L.): a review. Chemosphere 335, 139010. https://doi.org/10.1016/j.chemosphere.2023.139010.

Sheijany, M.S.P., Shariati, F., Mahabadi, N.Y., Karimzadegan, H., 2020. Evaluation of heavy metal contamination and ecological risk of soil adjacent to Saravan municipal solid waste disposal site, Rasht, Iran. Environ. Monit. Assess. 192, 757. https://doi.org/10.1007/s10661-020-08716-1.

Smith, E., Naidu, R., Weber, J., Juhasz, A.L., 2008. The impact of sequestration on the bioaccessibility of arsenic in long-term contaminated soils. Chemosphere 71, 773–780. https://doi.org/10.1016/j.chemosphere.2007.10.012.

Smith, E., Kempson, I.M., Juhasz, A.L., Weber, J., Rofe, A., Gancarz, D., Naidu, R., McLaren, R.G., Gräfe, M., 2011. In vivo–in vitro and XANES spectroscopy

assessments of lead bioavailability in contaminated periurban soils. Environ. Sci. Technol. 45, 6145–6152. https://doi.org/10.1021/es200653k.

Somani, M., Datta, M., Ramana, G.V., Sreekrishnan, T.R., 2020. Contaminants in soil-like material recovered by landfill mining from five old dumps in India. Process Saf. Environ. Protect. 137, 82–92. https://doi.org/10.1016/j.psep.2020.02.010.

Tyszka, R., Pietranik, A., Kierczak, J., Ettler, V., Mihaljevič, M., Medyńska-Juraszek, A., 2016. Lead isotopes and heavy minerals analyzed as tools to understand the distribution of lead and other potentially toxic elements in soils contaminated by Cu smelting (Legnica, Poland). Environ. Sci. Pollut. Res. 23, 24350–24363. https://doi.org/10.1007/s11356-016-7655-4.

USEPA, 2021. Guidance for sample collection for in vitro bioaccessibility assay for arsenic and lead in soil and applications of relative bioavailability data in human health risk assessment. https://semspub.epa.gov/work/HQ/100002712.pdf.

USEPA, 2022. ProUCL: statistical software for environmental applications for data sets with and without non-detect observations, Version 5.2. https://www.epa.gov/land-research/proucl-software.

Varol, M., Sünbül, M.R., Aytop, H., Yılmaz, C.H., 2020. Environmental, ecological and health risks of trace elements, and their sources in soils of Harran Plain, Turkey. Chemosphere 245, 125592. https://doi.org/10.1016/j.chemosphere.2019.125592.

Vongdala, N., Tran, H.D., Xuan, T.D., Teschke, R., Khanh, T.D., 2019. Heavy metal accumulation in water, soil, and plants of municipal solid waste landfill in Vientiane, Laos. Int. J. Environ. Res. Publ. Health 16, 22. https://doi.org/10.3390/ijerph16010022.

Wang, S., Han, Z., Wang, J., He, X., Zhou, Z., Hu, X., 2022. Environmental risk assessment and factors influencing heavy metal concentrations in the soil of municipal solid waste landfills. Waste Manage. (Tucson, Ariz.) 139, 330–340. https://doi.org/10.1016/j.wasman.2021.11.036.

Wei, Y., Shimaoka, T., Saffarzadeh, A., Takahashi, F., 2011. Mineralogical characterization of municipal solid waste incineration bottom ash with an emphasis on heavy metal-bearing phases. J. Hazard Mater. 187, 534–543. https://doi.org/10.1016/j.jhazmat.2011.01.070.

Wu, Y., Lou, J., Sun, X., Ma, L.Q., Wang, J., Li, M., Sun, H., Li, H., Huang, L., 2020. Linking elevated blood lead level in urban school-aged children with bioaccessible lead in neighborhood soil. Environ. Pollut. 261, 114093 https://doi.org/10.1016/j.envpol.2020.114093.

Wu, G., Wang, L., Yang, R., Hou, W., Zhang, S., Guo, X., Zhao, W., 2022. Pollution characteristics and risk assessment of heavy metals in the soil of a construction waste landfill site. Ecol. Inf. 70, 101700 https://doi.org/10.1016/j.ecoinf.2022.101700.

Wu, M.W., Dong, W.J., Guan, D.X., Li, S.W., Ma, L.Q., 2024. Total contents, fractionation and bioaccessibility of nine heavy metals in household dust from 14 cities in China. Environ. Res. 243, 117842 https://doi.org/10.1016/j.envres.2023.117842.

Xie, K., Xie, N., Liao, Z., Luo, X., Peng, W., Yuan, Y., 2023. Bioaccessibility of arsenic, lead, and cadmium in contaminated mining/smelting soils: assessment, modeling, and application for soil environment criteria derivation. J. Hazard Mater. 443, 130321 https://doi.org/10.1016/j.jhazmat.2022.130321. Part B.

Xu, D.M., Fu, R.B., 2022. The mechanistic understanding of potential bioaccessibility of toxic heavy metals in the indigenous zinc smelting slags with multidisciplinary characterization. J. Hazard Mater. 425, 127864 https://doi.org/10.1016/j.jhazmat.2021.127864.

Yang, S., Sun, L., Sun, Y., Song, K., Qin, Q., Zhu, Z., Xue, Y., 2023. Towards an integrated health risk assessment framework of soil heavy metals pollution: theoretical basis, conceptual model, and perspectives. Environ. Pollut. 316 (Part 2), 120596 https://doi.org/10.1016/j.envpol.2022.120596.

Zhou, P., Zeng, D., Wang, X., Tai, L., Zhou, W., Zhuoma, Q., Lin, F., 2022. Pollution levels and risk assessment of heavy metals in the soil of a landfill site: a case study in Lhasa, Tibet. Int. J. Environ. Res. Publ. Health 19, 10704. https://doi.org/10.3390/ijerph191710704.

Zwolak, A., Sarzyńska, M., Szpyrka, E., Stawarczyk, K., 2019. Sources of soil pollution by heavy metals and their accumulation in vegetables: a review. Water Air Soil Pollut. 230, 164. https://doi.org/10.1007/s11270-019-4221-y.